

Air Bearing Upgrade for Split Hopkinson Pressure Bar Experiment

Senior Design Final Report – April 2012

By

Donald Hayes II¹, Joseph Chason¹, Sarah Napier^{1,2}, Zachary Johnson^{1,3}

¹*Department of Mechanical Engineering*

²*National High Magnetic Field Laboratory*

³*Applied Superconductivity Center*



Project Sponsor

Joel W. House Ph.D.
AFRL/RWMWS



Project Advisor

Erica Cosmutto
Graduate Student FAMU-FSU College of Engineering

Department of Mechanical Engineering
FAMU-FSU College of Engineering
2525 Pottsdamer St, Tallahassee, FL 32310

Table of Contents

Abstract.....	6
1 Introduction	7
1.1 Introduction to Project.....	7
1.2 Needs Statement	8
1.3 Problem Description.....	8
1.4 Goal Statement	9
1.5 List of Objectives	9
1.6 Testing Environment	9
1.7 List of Constraints	10
1.8 Functional Diagram.....	11
1.9 QFD (house of quality)	12
1.10 Project Plan (Gantt chart).....	13
2 Concept Generation (All concepts)	14
2.1 Striker Bar Mechanism –.....	15
2.2 Incident and Transmitted Bars/ Air Bushings –.....	16
2.3 Base –	18
2.4 Data Acquisition/ Air Supply –.....	19
2.5 Strain Gauges –	19
2.6 Momentum Trap –.....	21
2.7 Bushing Alignment –	22
3 Final Concept (See Guidelines).....	23
4 Budget and Expenditures.....	25
5 Results and Discussion	27
6 Environment Health and Safety.....	29

7	Conclusions	30
8	Acknowledgements	31
9	Appendix	32
9.1.1	Detailed Budget	32
9.1.2	Stiker Bar Velocity Calculations	33
9.1.3	Comsol Analysis	35
9.1.4	Solenoid Optimization	45
9.1.5	Mathematics and Analysis Methods	46
10	Engineering Drawings	52
11	References	61
12	Biographies	64

Table of Figures

Figure 1 – Fall semester Gantt chart	Error! Bookmark not defined.
Figure 2 – Spring semester Gantt chart.....	Error! Bookmark not defined.
Figure 3 – Pendulum striker concept	Error! Bookmark not defined.
Figure 4 – Solenoid striker concept	Error! Bookmark not defined.
Figure 5 – Air bushings.....	Error! Bookmark not defined.
Figure 6 – Steel bars	Error! Bookmark not defined.
Figure 7 – I beam	Error! Bookmark not defined.
Figure 8 – T slotted framing	Error! Bookmark not defined.
Figure 9 – Foil strain gauge	20
Figure 10 – Semiconductor strain gauge	20
Figure 11 – Custom momentum trap	21

Figure 12 – Manufactured bumper	21
Figure 13 – Exterior alignment.....	Error! Bookmark not defined.
Figure 14 – Axial Alignment	Error! Bookmark not defined.
Figure 15 – Final design	Error! Bookmark not defined.
Figure 16 - Striker mechanism.....	Error! Bookmark not defined.
Figure 17 – Bars, gauges and sample.....	Error! Bookmark not defined.
Figure 18 – Air bushing	Error! Bookmark not defined.
Figure 19 – Custom momentum trap	Error! Bookmark not defined.
Figure 20 – Expenditures	26
Figure 21 – Strain plot	27
Figure 22 – Strain plot: areas under the waves	28
Figure 23 – Simplified graphic of Kolsky bar experiment	38
Figure 24 – Fully scaled Comsol image of Kolsky bar before loading	39
Figure 25 – Detail of sample and interface with incident and transmitter bars	39
Figure 26 – Detail of momentum trap.....	40
Figure 27 – Stress in the incident bar, specimen and transmitter bar w/static loading.....	41
Figure 28 – Stress in the incident bar, specimen and transmitter bar	42
Figure 29 – Deflection in the incident bar	43
Figure 30 – Stress developed in the momentum trap.....	43
Figure 31 – Wheatstone bridge	50

Table of Tables

Table 1 - Striker bar mechanism decision matrix.....	16
Table 2 - Incident and transmitted bar decision matrix.....	17
Table 3 - Air bushing decision matrix.....	17
Table 4 - Base decision matrix.....	18
Table 5 - Strain gauges decision matrix.....	21
Table 6 - Momentum trap decision matrix.....	22
Table 7 - Bushing alignment decision matrix.....	23
Table 8 - Budget.....	25
Table 9 - Areas under the strain waves.....	28

Abstract

Split – Hopkinson pressure bar (SHPB or Hoppy bar) systems are used to test the stresses and strains in material specimens in order to cause plastic deformation. The system begins with a striker bar mechanism which sets the system in motion. The striker bar is ejected out of a barrel with a constant, repeatable velocity until it comes in contact with an incident bar. This contact generates a wave, ideally in the form of a square pulse, which travels through the incident bar and comes into contact with the material specimen. At this point, the wave pulse splits in two. One pulse is reflected back through the incident bar while the other passes through the specimen, causing it to plastically deform, and into the transmitter bar. The transmitter bar is then set in motion and is stopped by a momentum trap, which removes the remaining energy from the test system. Strain gauges are placed on both the incident and transmitted bars near the material sample. A data acquisition system is attached to the strain gauges in order to record the pulse passing through the bars to see the plastic deformation trend of the specimen.

The air bearing upgrade for the split-Hopkinson pressure bar (SHPB) system, which has been designated to this group, is sponsored by Dr. Joel House at the Eglin AFB Research Laboratory. The task is to research upgrades to the air bearings that are currently used on the 0.625” diameter split-Hopkinson pressure bar at Eglin and produce a small scale SHPB system. To decide which air bearings would best suit the SHPB, research of the current selection of commercial air bearing companies was conducted, and factors such as cost, availability, and efficiency were explored. At Eglin, the current SHPB system utilizes standard journal bearings to allow the incident and transmitted bars to move. The major drawback of these bearings is the inherent friction introduced into the system by their use. It was the intention of this project to investigate the use of air bushings on a portable, small scale SHPB. The following report contains the research, calculations, component selection, construction, and testing done in order to produce such a system by the end of the spring semester of 2012.

1 Introduction

1.1 Introduction to Project

In 1914, Bertram Hopkinson came upon a method by which a metal bar could be used to test stress pulses. In 1949, H. Kolsky used Hopkinson's idea and expanded upon it. He devised an experiment using two collinear bars to measure stress and strain through a material sample, known today as the split-Hopkinson pressure bar experiment.

In this experiment, a specimen is placed between the two collinear bars called the incident and transmitter bars. These bars are placed in linear bearings and are equipped with strain gauges. A device at one end of the incident bar is used to set the bar in motion and create an incident strain wave. The transmitter bar then presses against and deforms the specimen. The energy which passes through the sample and into the transmitter bar is removed from the system by a momentum trap constructed from a shock absorbing material.

When the incident wave passes through the incident bar to the specimen, it is split into two waves as it reaches the specimen. The first is called the transmitted wave and passes through the specimen, plastically deforming it. The second is called the reflected wave and reflects from the specimen back through the incident bar. The stress and strain felt by the deformed specimen can be calculated based on the information collected from the strain gauges as the waves pass through the two bars.

The bar diameter can vary in size; 5/8 in. and 2 in. diameters are used at the Eglin Air Force Research Lab. In order for the waves to move precisely through the bars, it is important that they be precisely aligned. This alignment is a critical task that must be correctly conducted for the apparatus to work properly.

Located along a split-Hopkinson bar are several bearings. As was stated before, this project involves the upgrading of the existing journal bearings currently used on the SHPB at Eglin, to air bearings. Air bearings function by providing a thin, pressurized film of air that is nearly frictionless. This film of air allows bars to move freely and with little friction. There must be a slight size difference between the bearing and the bar, so

that the bars will not come in physical contact with the bearings. The placement of the air bearings must not interfere with the placement of the strain gauges so as to not deter the accuracy of the strain data.

1.2 Needs Statement

Warhead design engineers and material scientists require mechanical property information under high deformation rates of loading on a wide variety of materials that have military significance. The most generally accepted technique for gathering such information is the SHPB experiment. The Air Force Research Laboratory's Damage Mechanisms Branch has operated such an experiment for approximately 30 years. The Damage Mechanisms Branch has a requirement to replace the current bearing system with a new air bearing design.

1.3 Problem Description

As was previously mentioned, in addition to selecting the air bearings for the Eglin SHPB, this group was asked to produce a portable prototype at the FAMU/FSU College of Engineering to represent the larger SHPB at Eglin's Research Lab. One of the project's first major decisions was to establish the diameter of the bars and bushings which would be best to implement on the small scale SHPB; this would directly affect its weight, and therefore its portability. Another less obvious issue was determining how the SHPB apparatus should be kept rigid during testing. Further decisions to be made included: determining what type of mechanism would be most appropriate for striking the incident bar to produce strain; devising a procedure to align the bushings to the necessary level of precision; deciding on the type of strain gauges to be used; the type of air supply for the bushing system; obtaining access to a Data Acquisition System (DAQ) capable of the high data acquisition speeds required for testing.

1.4 Goal Statement

The goal of this project is to research upgrades for the current bearing system utilized on the split-Hopkinson pressure bar experiment in the Air Force Research Laboratory's Damage Mechanism Branch at Eglin AFB and produce a small scale SHPB to demonstrate the effectiveness of the upgrades chosen.

1.5 List of Objectives

The most crucial objectives of this project are as follows:

- Analyze the engineering challenge of upgrading the Eglin AFB SHPB to a physical architecture based on the use of air bearings.
- Provide analysis of air bearing hardware cost, interface requirements, installation procedures and impact on the bar geometry.
- Provide an assessment of strain gauge technology.
- Develop a procedure to align the bars based on the new architecture.

Other objectives of the project are the acquisition of suitable bearings and related equipment, the installation of the new bearing system on the SHPB, and the initial testing of the SHPB.

1.6 Testing Environment

The prototype was tested in the thermal fluids laboratory at the FAMU/FSU College of Engineering, which had the DAQ system necessary for testing. The test setup consisted of the prototype being set on a table that covered its entire length for maximum support during testing. The air bushings were supplied with argon gas at roughly 60 psi from an argon tank rated at 4000 psi.

It was mandatory to do leak testing on the physical device to see if the air bushings were fully functioning in which the bars would float on the surrounding argon. Also, the

testing of the solenoid and the switch were vital so that the SHPB would be able to operate upon the flipping of the switch.

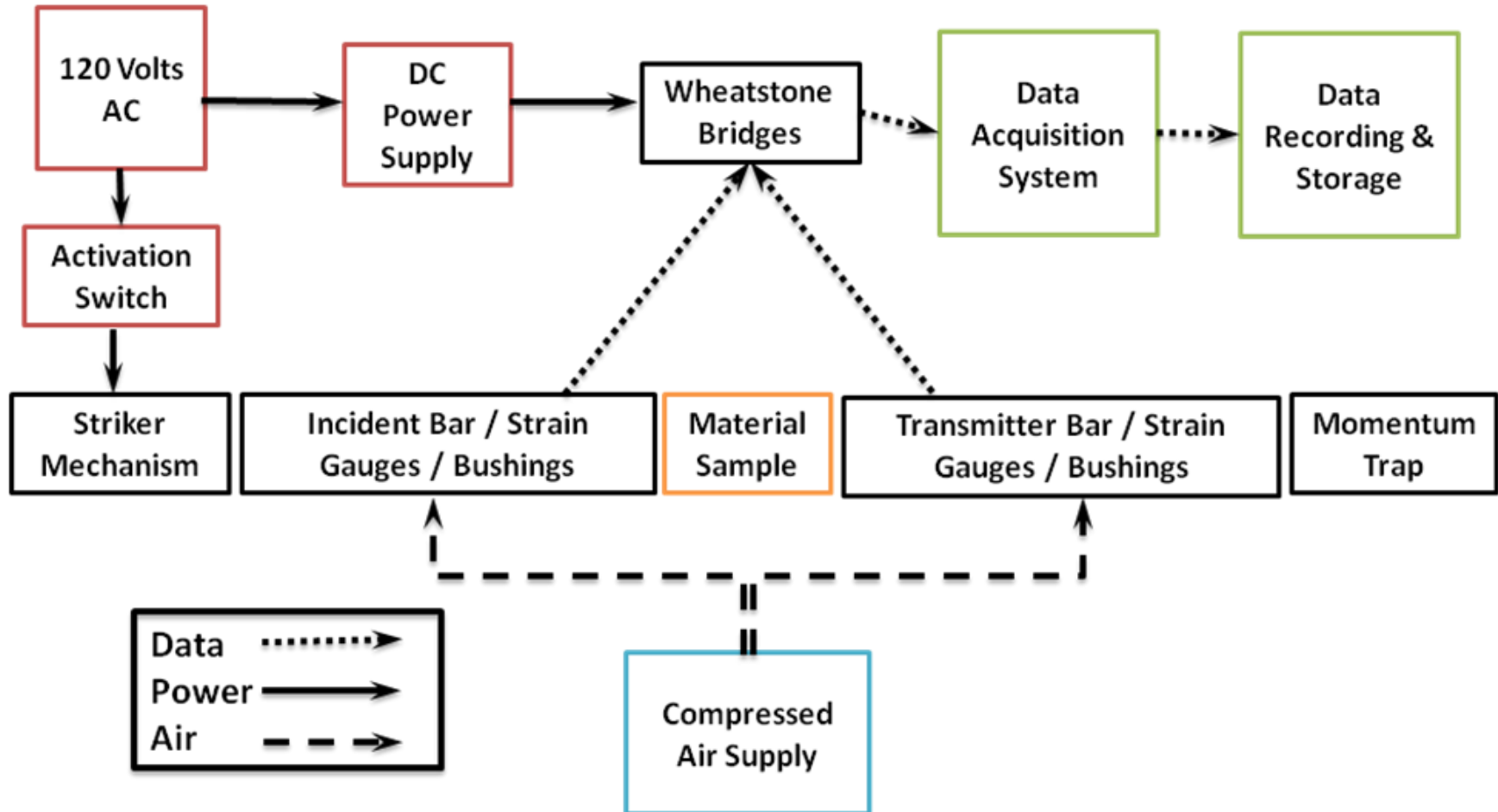
Another one of the main aspects of the experiment involved obtaining strain data from the data acquisition device. The written LabView program was tested to see if a reading could be obtained from the program in the form of a square pulse wave. It was calculated that the data acquisition was to have a speed capable of at least 100 Hz to ensure a sufficient amount of data points for generating a usable strain plot. The data acquisition used in the thermal fluids lab was capable of 125 mega samples per second, which was divided among two channels for the strain data to be recorded from the incident and transmitted bars.

1.7 List of Constraints

Several constraints were given by our sponsor for the development of the SHPB prototype. The constraints include the following:

- The project must remain within a \$2500 budget.
- The prototype must consist of a smaller table top version of the system with 5/8" diameter bars currently at Eglin.
- The bars and air bearings must be selected based on a workable size.
- A striker mechanism for the system must be selected to acquire plenty of velocity to initiate high impact between the incident and transmission bars.
- A device must be created to stop the system after impact.
- An air supply system must be selected to consistently supply clean air to the air bushings.
- A strain gauge wiring schematic must be chosen in order to achieve accurate results.
- The data acquisition device must be compatible with the strain gauge set up and must possess a sufficient amount of speed.

1.8 Functional Diagram



1.9 QFD (house of quality)

Column #	1	2	3	4	5	6	7	8	9	10
Max Rating	9	3	3	9	9	1	3	9	9	9
Weight	500.0	150.0	150.0	600.0	630.0	50.0	180.0	600.0	450.0	470.0
Relative Weight	13.23	3.97	3.97	15.87	16.67	1.32	4.76	15.87	11.9	12.43
Limit or Target Value	< \$2500	< 50 lb.	"Table Top" Version	2 Person Carry

Row #	Max Rating	Relative Weight	Weight	Primary Requirements	1	2	3	4	5	6	7	8	9	10
				Secondary Requirements	Cost	Weight	Size	Simplicity	Durability	Portability	Scalability	Accuracy	Data Quality	Ease of Use
1	9	50.0	50.0	Analyze SHPB design based on use of air bearings	9	3	3	9	9	1	3	3		9
2	9	20.0	20.0	Assess strain gauge technology	1			3	9			9	9	1
3	9	30.0	30.0	Develop procedure to align bars	1			3			1	9	9	

1.10 Project Plan (Gantt chart)

Senior design group 1 was given two semesters to complete this project where the teams were assigned during early September in 2011. In general, the team designed the prototype in the fall semester and built and tested the prototype in the spring semester.

The design schedule is shown below in figure 1. The team worked well through all aspects of the design phase. A small two week set back in purchasing was the only known issue during this phase due to a glitch in communication between team members, but was quickly resolved. All other issues were handled well within the designated time scheduled for.

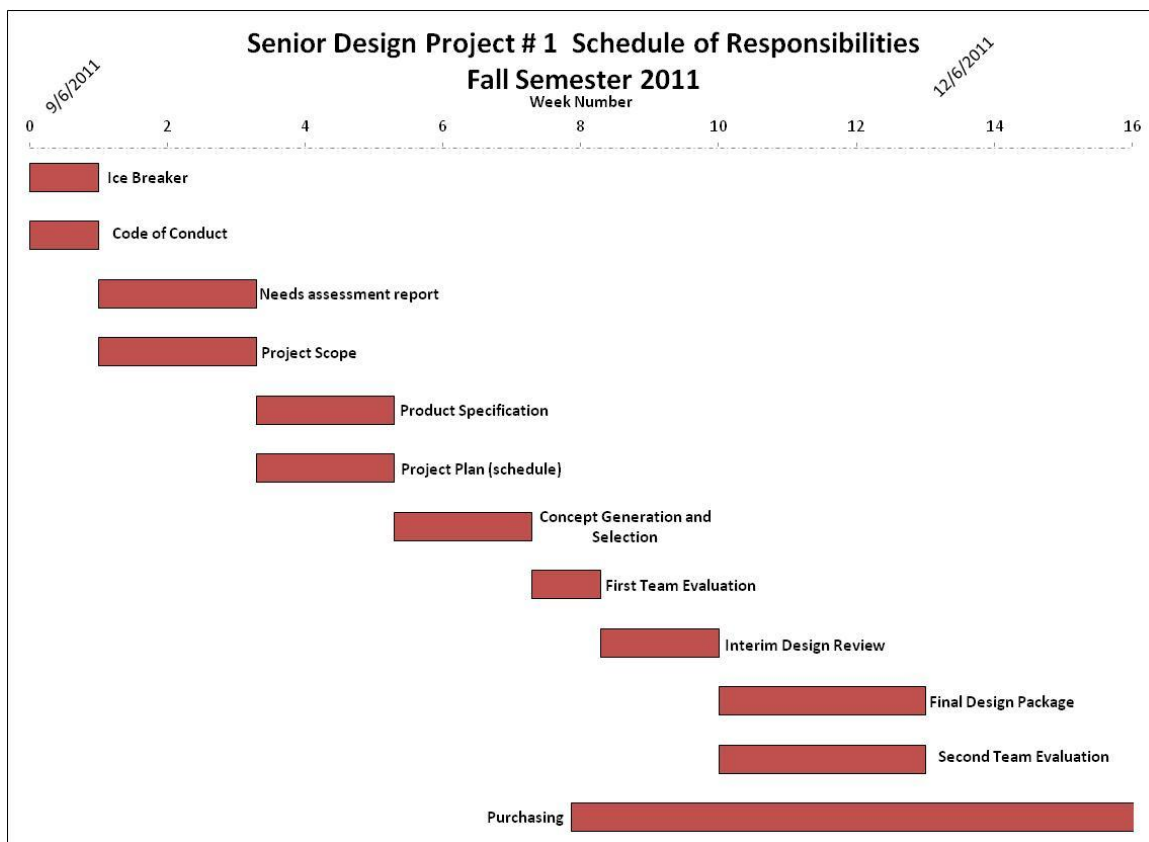


Figure 1 – Fall Semester Gantt chart

The building and testing schedule from the spring semester is shown below in figure 2. The team got off to a deliberate start, preferring to have all parts acquired and machined before final assembly, in case of difficulties. The largest issue encountered during the build phase was

slight rusting on the bars—easily removed with fine grit sand paper—and the low sampling rate of the data acquisition system.

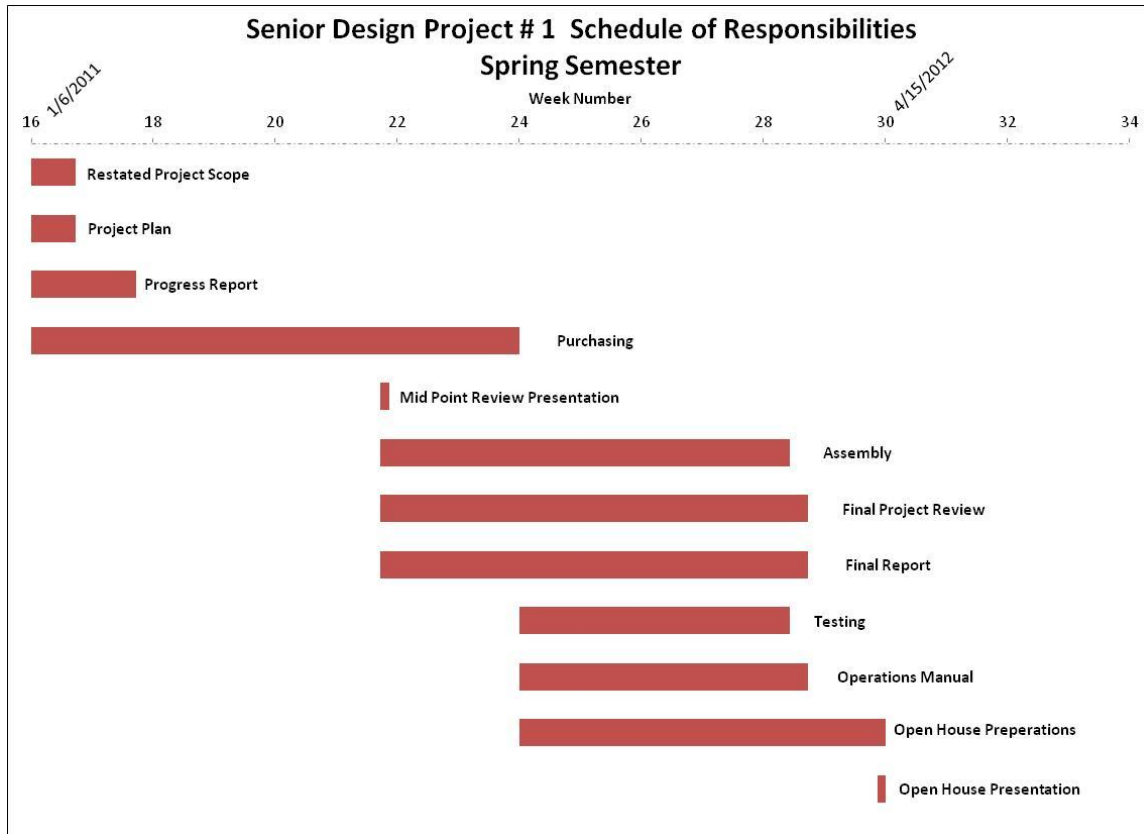


Figure 2 – Spring semester Gantt chart

2 Concept Generation (All concepts)

In order to efficiently generate the design of the final SHPB prototype, the experiment was broken into subsections. Each section was studied, multiple concepts were produced, and from those concepts the final design choices were made. The physical subsections of the experiment were chosen to be the:

- Base
- Striker Bar Mechanism

- Bars and Air Bushings
- Strain Gages
- Momentum Trap
- Air Supply Manifold

In addition to the physical architecture of the design, a method of aligning the bushings to the proper tolerances as well as the data acquisition system to be used during testing needed to be determined. For each of these areas, the two most adequate concepts were also selected and chosen from.

2.1 Striker Bar Mechanism -

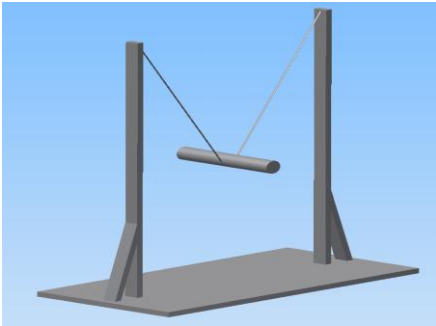


Figure 3 - Pendulum Striker

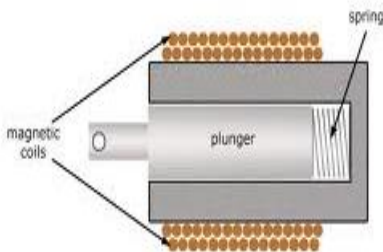


Figure 4 - Solenoid Striker

For the striker mechanism, the choice of designs came down to building a pendulum hammer or using an electric solenoid to propel a striker bar. The benefits of the pendulum hammer are that it is a cheap, mechanical way of producing a shockwave in the bars. The entire mechanism would cost less than \$50 in materials however, its design would require a large hammer mass to cause a strain high enough to deform a sample. Also, given that the hammer would be suspended by ropes or cables, assuring a proper impact between it and the incident bar could prove difficult. On the other hand, an electric solenoid would be able to consistently propel a striker bar at a known speed.

By constraining the bar within a PVC tube, its impact with the incident bar could be controlled. A solenoid capable of producing enough force to drive a 0.75 inch diameter striker bar to the required speeds costs between \$60 and \$100. Since the cost is not significantly greater and the velocity of the striker bar can be more easily controlled, it was decided that the final design would implement a solenoid as the striker bar mechanism.

Table 1 - Striker bar mechanism decision matrix

	<u>Weight</u>	<u>Pendulum Hammer</u>	<u>Electric Solenoid</u>
<u>Cost</u>	0.2	4	3
<u>Simplicity</u>	0.2	5	3
<u>Accuracy</u>	0.3	3	5
<u>Durability</u>	0.2	4	5
<u>Weight</u>	0.1	4	4
<u>Weighted Score</u>	1.0	3.9	4.1

2.2 Incident and Transmitted Bars/ Air Bushings -

Since the size of the incident and transmission bars would directly determine the size of the air bushings, and vice versa, the bars and bushings were considered in parallel. The choices of diameter of the bars and bushing were narrowed to 0.5 inch and 0.75 inch options because of overall size, cost, and availability. The final choices of these components came after some analysis of the striker bar mechanism. It was mathematically determined that by using 0.75 inch diameter bars, producing the amount of strain required to deform a copper sample would be more easily

achieved. This also would benefit the group during the spring 2012 semester when strain gages must be applied to the bars. It is believed that the larger the diameter of the bars, the easier the application of the strain gages will be.

As for the costs of the bushings, New Way Air Bearings and Nelson Air Corporation were contacted about the prices and specifications of their products for comparison and decision making. In both price and robustness, New Way Air Bearing's products were seen to be



Figure 5 - Air Bushings



Figure 6 - Steel Bars

superior. New Way bushings cost approximately \$50 less than those of Nelson Air Corp. while supporting 50% more radial load. Using McMaster-Carr, the price difference between bars of 0.5 and 0.75 inches in diameter would not be an issue. Precision 1566 steel shafts cost \$20 and \$30 for 0.5 and 0.75 inch diameter bars, respectively. As is shown by the decision matrices below, it was decided to implement 0.75 inch diameter air bushings and bars in the final design.

Table 2 - Incident and transmitted bar decision matrix

	<u>Weight</u>	<u>0.5" diameter</u>	<u>0.75" diameter</u>
<u>Cost</u>	0.1	4	3
<u>Weight</u>	0.2	4	4
<u>Size</u>	0.1	5	5
<u>Durability</u>	0.2	5	5
<u>Portability</u>	0.1	4	4
<u>Accuracy</u>	0.2	3	4
<u>Data Quality</u>	0.1	3	4
<u>Weighted Score</u>	1.0	4.0	4.2

Table 3 - Air bushing decision matrix

	<u>Weight</u>	<u>New Way</u>	<u>Nelson Air</u>
<u>Cost</u>	0.2	3	2

<u>Weight</u>	0.2	5	5
<u>Size</u>	0.1	5	5
<u>Durability</u>	0.2	5	4
<u>Portability</u>	0.1	5	5
<u>Accuracy</u>	0.2	5	4
<u>Weighted Score</u>	1.0	4.6	4

2.3 Base -

The choice for constructing the prototype's base came down to using an I-beam or constructing a foundation using T-slotted framing. The I-beam would cost less than \$100, it would have high strength, its design would allow for simple alignment of the bushings, and it would be completely scalable.

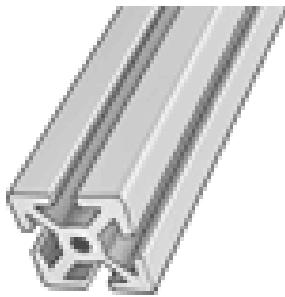


Figure 8 - T-slotted Framing

However, due to the size of an I-beam, its weight could cause the portability of the design to be reduced. On the other hand, the T-slotted framing would require around \$120 worth of material to construct

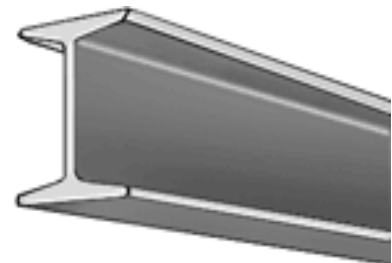


Figure 7 - I-Beam

the base, would be lightweight, its geometry would allow it to create a very rigid base, and its scalability is excellent. As can be seen in the decision matrix below, the T-slotted framing was chosen to be best for

use in the design.

Table 4 - Base decision matrix

	<u>Weight</u>	<u>I - Beam</u>	<u>T-Slot</u>
<u>Cost</u>	.3	3	5

<u>Simplicity</u>	.2	4	4
<u>Weight</u>	.2	2	4
<u>Portability</u>	.3	4	5
<u>Weighted Score</u>	1.0	3.3	4.6

2.4 Data Acquisition/ Air Supply -

The choices of data acquisition system and air supply manifold type were not as crucial at this stage of the project as the choice of the other sections. Early on it was decided that the air manifold would be composed of a 4 to 6 foot long steel pipe which used flexible tubing to deliver air to the individual bushing blocks. The main air supply would come either from a compressor or a pressurized tank of air. The pipe would have a purge valve as well as shut off valves for each of the bushings to ensure that if liquid or other contaminants were to make their way into the manifold, a method of isolating the bushings and flushing the system would be available. The only choice to be made was to either set the manifold at an incline or to lay it horizontally. As the inclined version would simply complicate construction, the horizontal version was chosen. However, during construction it was found that simply using the flexible tubing would be sufficient and the metal tube was removed from the final design. The choice of data acquisition came down to deciding between LabVIEW and MatLab. At the FAMU/FSU College of Engineering, it was found that LabVIEW was the more available of the two options and was therefore chosen as the system to be used in the testing portion of the project.



2.5 Strain Gauges -

When researching types of strain gages to implement in the SHPB system, the two best options found were foil and semiconductor gages.

The companies which produce the foil and semiconductor gages in question are Vishay and Micron-Instruments, respectively. Foil strain gauges work due to the deformation of a strain sensitive pattern. This pattern is etched out of a metal foil and placed securely onto a backing.

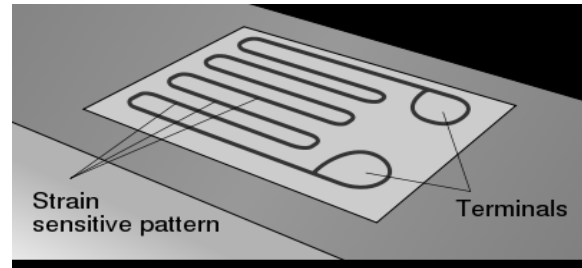


Figure 9 – Foil Strain Gage

Once firmly applied to a piece of material, deflection of that material is transferred to the foil pattern and a change in electrical resistance is caused. Semiconducting gages work by replacing the foil pattern with a doped semiconducting material which also responds to geometric changes with changes in electrical resistance. As for pros and cons, foil gages are durable, cost \$10 to \$20 each, and are a proven method of strain detection. Their only downside may be their low gage factor. Vishay foil gages have a factor of approximately 2. For those who do not know, gage factor is the measure of a gages response to a given amount of strain. The higher the gage factor, the higher the gage's response to a given amount of strain will be. Probably the greatest

Figure 10 – Semiconductor Strain Gage

benefit of semiconducting gages is that they exhibit higher gage factors than do foil gages. Micron-Instruments list their gages as having factors in the 140 range. This would allow for them to be used in situations where the amount of strain is so small as to not be detected using a foil gage or where foil gages do not provide high enough accuracy to correctly represent a strain pulse. However, a drawback to is that semiconductor gages do not have the durability of foil gages and are therefore are more easily damaged during installation and operation. As for cost, Micron-Instrument's semiconductor gages are also \$10to \$20 each if bought individually, but can cost between \$80 and \$160 for a matched set of 4 gages. In the decision matrix below, it is seen that the semiconducting gages were believed to be the better choice. However, Micron Instruments was contacted as to some of the specifications of their gauges and the intention of this project was discussed. For the purpose of this project, Micron-Instruments suggested the use of foil gages unless it was determined that the use of semiconducting gages was absolutely

required. Also, upon contact with Vishay it was found that student rates as low as 10 gauges for \$20 were available. Given this turn of events, foil gages will be used in the final design.

Table 5 - Strain gauges decision matrix

	<u>Weight</u>	<u>Foil</u>	<u>Semiconductor</u>
<u>Cost</u>	0.2	3	2
<u>Size</u>	0.1	5	5
<u>Data Quality</u>	0.2	5	4
<u>Durability</u>	0.1	5	5
<u>Ease of Use</u>	0.2	5	4
<u>Weighted Score</u>	1.0	4.6	4

2.6 Momentum Trap -

In order to maintain the functionality of an SHPB experiment, a device must be constructed that will decelerate the incident and transmission bars after a test has been run. This function is



Figure 12 - Manufactured Bumper

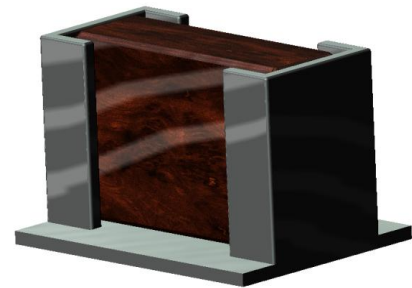


Figure 11 - Custom Momentum Trap

the purpose of the momentum trap. For this design, the requirements set up for the momentum trap are simply that it will have the ability to absorb the impact of the transmitter bar while having low cost. The two options which were chosen from were construction of a custom bumper or the use of a pre-made device. As for the benefits of both types, they are low cost, replaceable, and have the ability to absorb significant impacts. In the final decision, as seen in the decision matrix below, the choices were very close in all areas of concern. When the final decision was made, it was

determined that a custom trap would be the best choice because it is the most easily scaled of the two choices.

Table 6 - Momentum trap decision matrix

	<u>Weight</u>	<u>Custom</u>	<u>Prefabricated</u>
<u>Cost</u>	0.2	4	4
<u>Weight</u>	0.1	4	3
<u>Size</u>	0.1	3	3
<u>Simplicity</u>	0.1	4	4
<u>Durability</u>	0.25	4	3
<u>Scalability</u>	0.15	4	3
<u>Ease of Use</u>	0.1	4	4
<u>Weighted Score</u>	1.0	3.9	3.4

2.7 Bushing Alignment -

For the decision regarding bearing alignment, it was determined early on that some type of laser based alignment would be used to place the bushings

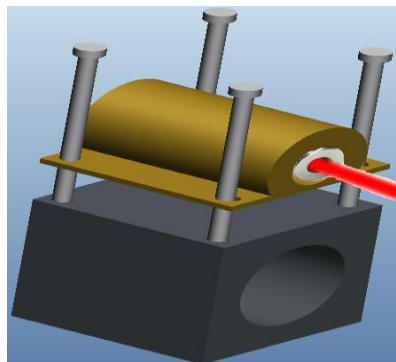


Figure 13 – Exterior Alignment

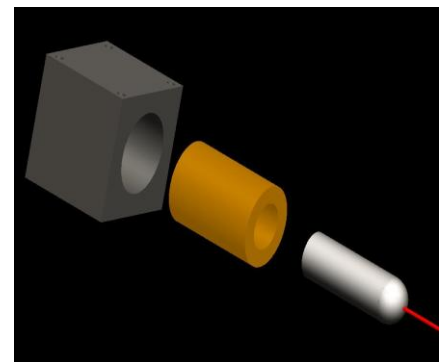


Figure 14 – Axial Alignment

in the correct relationship axially with one another.

The two methods which were chosen from were very similar. The major difference is that with one the laser would be mounted on the top of the bearing blocks and with the other it would be

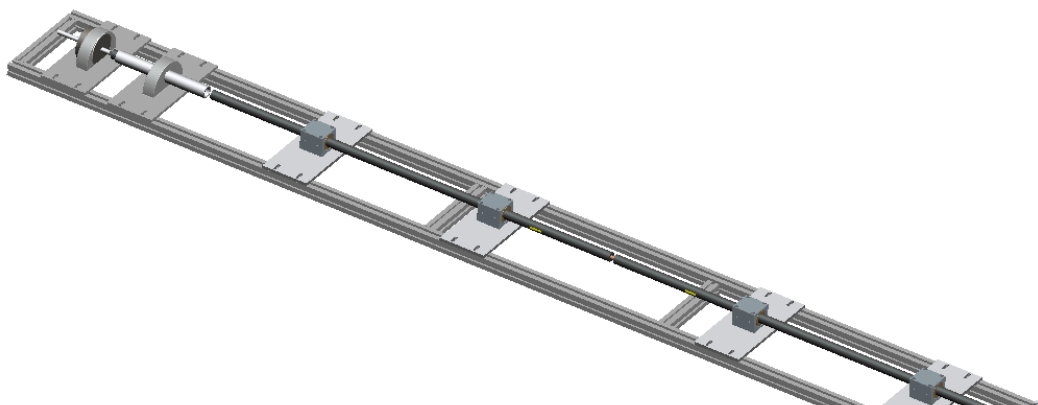
mounted in the center of the block. These choices were labeled as center-bore and exterior alignment. As can be seen below, the final choice of the group was to use the center bore alignment method. This method was chosen because of the accuracy with which the laser could be mounted relative to the bushing block's center axis. The alignment of the blocks was done with the laser being mounted within one block and a small target mounted within the next. When the laser illuminates the correct portion of the target insert, the two blocks will be aligned.

Table 7 - Bushing alignment decision matrix

	<u>Weight</u>	<u>Center-Bore</u>	<u>Exterior</u>
<u>Cost</u>	0.2	3	3
<u>Simplicity</u>	0.1	2	4
<u>Scalability</u>	0.2	4	3
<u>Accuracy</u>	0.4	5	4
<u>Ease of Use</u>	0.1	5	3
<u>Weighted Score</u>	1.0	4.1	3.5

3 Final Concept (See Guidelines)

By combining the final design choices, the overall design shown below was formed. It should be noted here that the air manifold system is not represented in this drawing in order to more clearly show the main components of the design. When mounted, the manifold would simply run parallel to the bars along the edge of the design



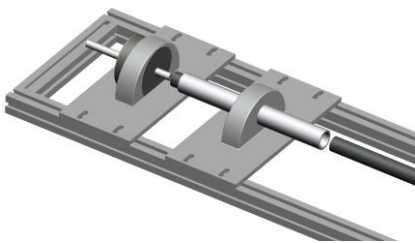


Figure 16 – Striker Mechanism

The picture to the left shows the striker mechanism of the final design consisting of a solenoid mounted in an aluminum cross-plate, a striker bar, and a guide tube to ensure correct alignment between the striker and incident bars during impact. This mechanism should provide consistent striker bar velocities and repeatable test conditions.



Figure 17 – Bars, Sample, and Strain Gages

Figure 16 shows the incident and transmitter bars with the strain gages in position, 6 inches from the ends of the bars where they meet. In the center of the two bars where they meet is the copper specimen to be plastically deformed upon impact. Each bar will be equipped with two strain gages for optimum results.

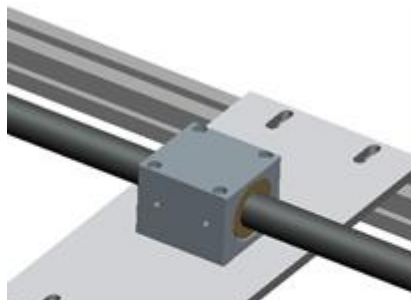


Figure 17 is a close up image of a single air bushing with the bushing block, bushing, and steel bar installed. There will be a total of 4 air bushings used in this design.

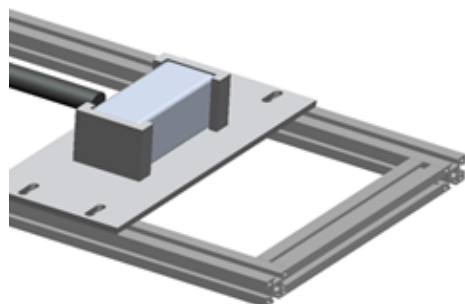


Figure 18 shows the custom momentum trap design which consists of a block of wood housed within U channel. This momentum trap will absorb the kinetic energy from the system.

Figure 19 – Custom momentum trap

4 Budget and Expenditures

Senior design team 1 was given a base budget of \$2,500. The total expenditures to date are \$2117.13. The team is well under budget by a total of \$382.87 or a total of 15% lower than allowable. The following chart shows the total expenditures of the team item by item.

Table 8 - Budget

Item	Quantity	Unit Cost	Total Cost
Solenoid	1	69.94	\$69.94
T-slot Framing 1 1/2 inch (96 inch length)	2	48.15	\$96.30
Incident & Transmission Bar: 1566 Steel Bar 0.75 inch (36inch length)	2	29.42	\$58.84
T-slot Framing 1 1/2 inch (4 foot length for 6 inch braces)	1	25.15	\$25.15
Air Manifold (72 inches)	1	16.34	\$16.34
Striker Bar: 1566 Steel Bar 0.75 inch (6inch length)	2	5.17	\$10.34
Right Angle Fastener	16	4.06	\$64.96
Fasteners (Packs of 4)	16	2.71	\$43.36
Strain Gauges (Pack of 10)	3	20	\$60.00
Air Bushings 0.75 inch	4	265	\$1,060.00
Bushing Block 0.75 ID	4	135	\$540.00
0.25"x3"x72" Aluminum Sheet	1	40.35	\$40.35
0.75" Diameter x 12" Long High Tolerance Aluminum Bar	1	12.1	\$12.10
12" Aluminum U-Channel	1	14.19	\$14.19
0.75" diameter x 6" Long High Tolerance Steel Bar	1	5.26	\$5.26
Total			\$2,117.13

Total Budget	\$2,500.00
Total Amount Under Budget	\$382.87
Percentage Under Budget	15.31%

T

able 8 above shows the allocation of all expenditures for the split-Hopkinson pressure bar project. The overwhelming expenditure of \$1600 was towards the air bushings themselves, which was of 79% of the total expenditures, but was deemed necessary as it was the main focus of the project. Lower cost options are available, however, Eglin’s existing upgraded Hopkinson bar experiment with 2 inch diameter bars, used very specific uniform lift air bushings from New Way Air Bearings.

Figure 19 given below shows a physical representation of the final allocation of the entire budget. The major purchase was that of the air bushings themselves. The project was an economic success as it came in 15% under the allowed budget. The additional materials –bars, framework, air supply, and other systems—amounted to the remainder of the expenditures at 20.8%.

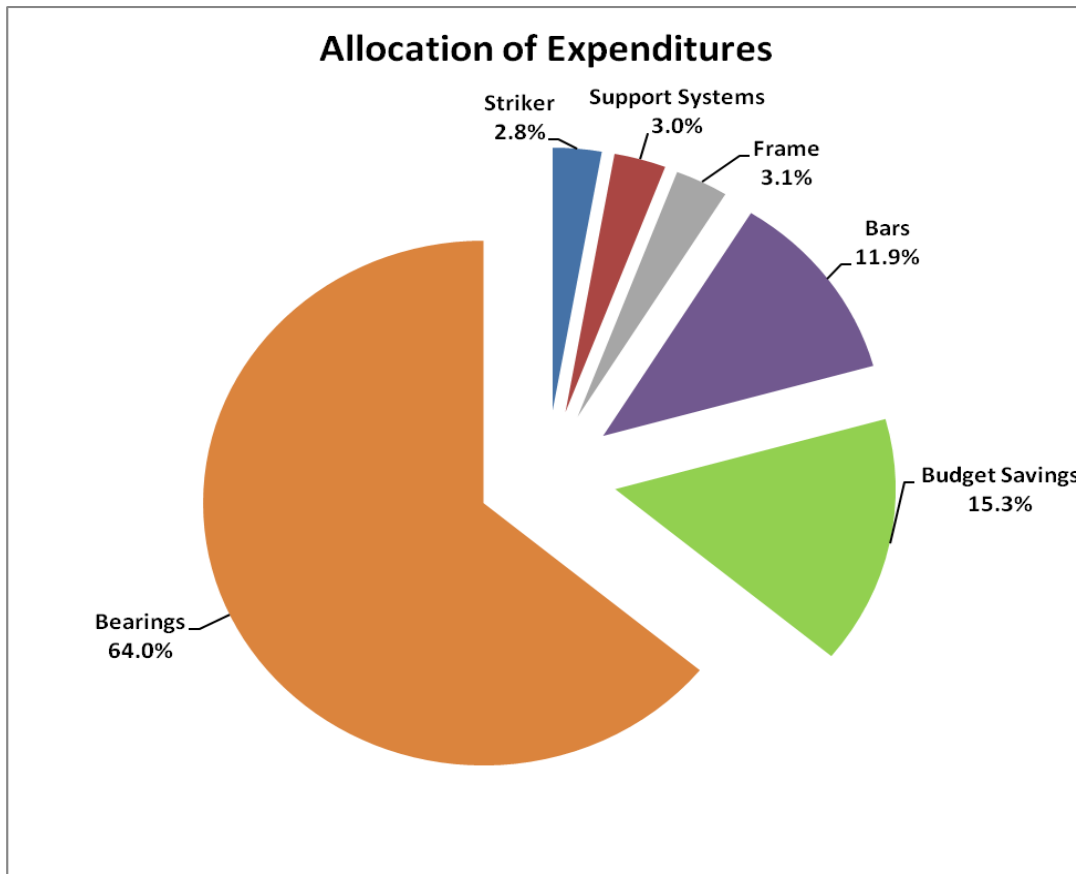


Figure 20 – Expenditures

5 Results and Discussion

The results of the testing were positive but not conclusive. The low sampling rate of 250 kHz gave a maximum strain wave measurement of 3 data points. In figure 20 below, an example of the impulse waves are given.

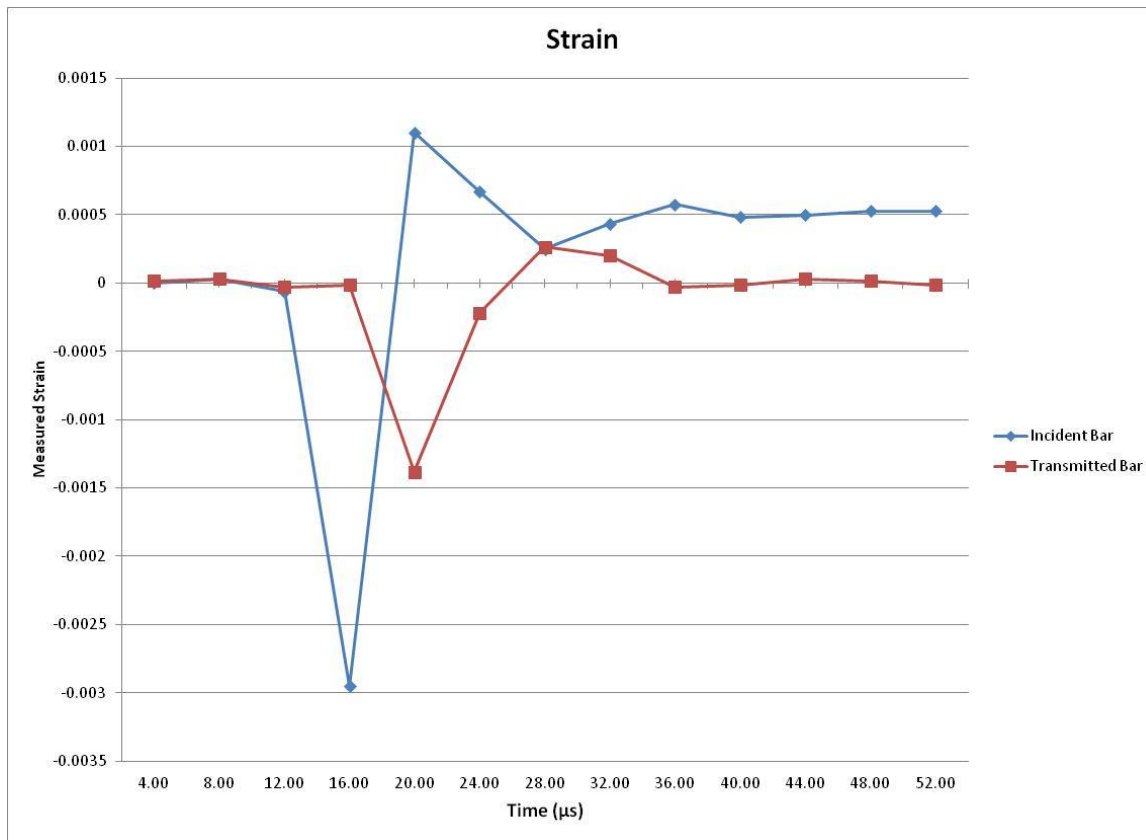


Figure 21 – Strain plot

The graph shows the lack of resolution necessary to give reliable data for a true strain rate test, but three desired waves are illustrated. In figure 21 shown below, each wave is labeled clearly.

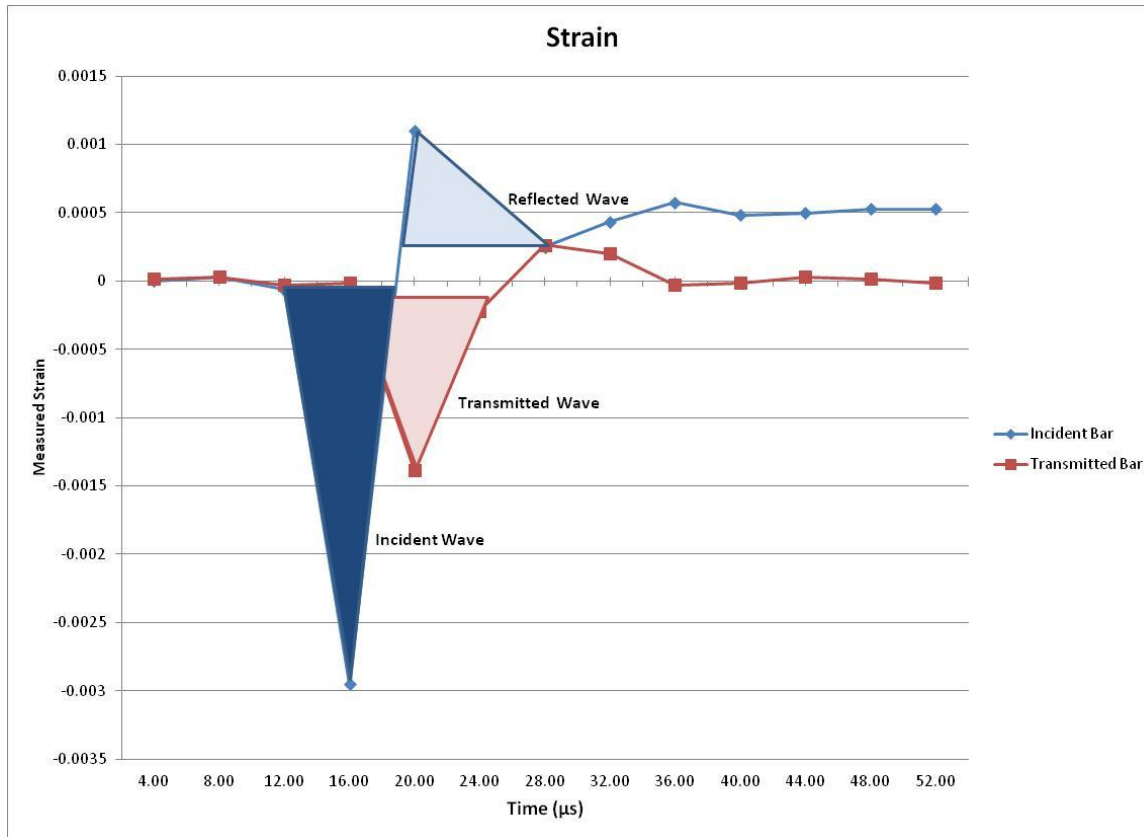


Figure 22 – Strain plot: areas under the waves

It is the kinetic energy in the area encompassed by the triangles which gives the energy absorbed by the sample. Table 9 shown below gives the basic calculation of the area under the curves. This table shows that the data acquisition system worked. The proof is that the difference between the initial pulse and the sum of both the reflected and transmitted pulse is a reasonable number. This difference is given as the “Absorbed” percentage.

Table 9 - Areas under the strain waves

$\int d\epsilon * ds$ (s)	Incident	Reflected	Transmitted	"Absorbed"
Strain-Seconds	1.15 E-08	4.47 E-09	5.46 E-09	
% of Initial Pulse	100.00%	38.71%	47.31%	13.98%

During all of the testing the copper specimen underwent no plastic deformation, which may be due to several factors. First, the solenoid chosen was the strongest available and gave

slightly more power than needed for plastic deformation. These calculations were done ignoring friction and other losses. Second, the copper samples themselves were not heat treated as was desired to have minimum strength, which would in turn have allowed the team to be able to measure the plastic strain energy. Lastly, there was a slight misalignment of the solenoid and striker bar, which may have caused absorption of energy via rotational inertia. It is believed that the main cause of elastic behavior in the copper was the lack of annealing done to the specimen. The “absorbed” percentage given in table 9 is representative of the large amount of error due to sampling rate issues.

The project may be heralded as a success. The design, component selection, fabrication, assembly, testing, and data reduction was all accomplished in a timely manner yielding in the final product being a mechanically operational split-Hopkinson pressure bar system.

6 Environment Health and Safety

The building and operation of the SHPB apparatus will cause no harm to the environment as there are no harmful fluids or release of radiation that could leak out into the surroundings. Therefore, there are no health hazards due to inhalation or skin contact of a substance in which case, this project can be said to be environmental friendly.

The safety measures that should be taken when transporting the SHPB include two people carrying the apparatus with both hands on the ends of the device. Also, extreme care should be taken when transporting the 4000 psi argon tank. It should not be dropped. The solenoid is capable of a velocity of 7 mph. Also, the forces generated to all of the bars could damage someone’s finger. A certain amount of distance should be kept from the apparatus when in operation to ensure that safety is maintained. If a metal specimen is being tested, caution should also be taken because of the possibility of the specimen flying out after the impact of the bars. It may be necessary to cover the region where the specimen is located between the bars with a box of safety to prevent specimen fragments from possibly shooting out from between the bars, or slammed down on the ground due to its high pressurization.

Another set of safety measures are required when the SHPB device is in operation. No hands should be on any part of the prototype after the solenoid is released.

7 Conclusions

The SHPB system is used for testing material properties in warheads for military purposes. Despite the main goal of this project, which was to upgrade the current journal bearings to air bearings on the SHPB at the Eglin Air Force Base, the task of building a smaller working prototype was successfully completed. The 8 foot long prototype showed the basic functionalities of the 45 foot long SHPB at Eglin. Not only was the physical working system displayed, but sufficient data from the strain gauges were generated.

The design phase of the prototype was a critical moment in the success of the project. After the concept generation process, the final design model was developed based on the overall structure and the individual components that would achieve the best results. The base had to be sturdy in order support the system during testing as well as lightweight so that it could be transported by one or two individuals. The base material composed of T-slotted framing, was the best candidate for this application. In order to initiate the device, a solenoid was used as the striker mechanism to produce constant velocity. The solenoid was controlled by the flip of a switch to set the system in motion. The incident and transmitter bars and air bushing sizes were essential because the bars provided a means for the pulse waves to travel. Also, the bars had to be large enough for the strain gauges to be mounted on. Due to the size, cost, and availability the bar and bushing sizes were 0.75 inch diameter. The bushing alignment system worked flawlessly and the bushings were aligned with high precision. The air supply system consisted of the use of argon gas because of its being clean and pure. In order to achieve strain data, the strain gauges were a highly contributing factor. Foil strain gauges were the best solution because of their durability and relative ease of mounting being that the team had little experience with mounting strain gauges. The strain data was measured on a computer via LabView, which required the use of an efficient data acquisition system. Labview was chosen because of its familiarity in industry. The data acquisition had to be considerably fast in providing results at a speed of at least 100 Hz.

The testing of the SHPB prototype provided satisfying results. It achieved the goal of generating spikes from the impact of the bars with a low error of 14% from the absorbed energy within the specimen. Several runs were conducted in which some were conducted with no specimen in between the incident and transmission bars. The other runs involved the copper specimen in between the bars, but the specimen was unsuccessfully plastically deformed. The results from testing the prototype were compared to the results given from the SHPB at the Eglin Air Force Base. The test data was not the most reliable, but there were some respectable aspects from the data. For testing the copper specimen, receiving non-plastic deformation of the sample was not expected. However, this problem can be easily fixed by choosing a less powerful solenoid and annealing the copper to increase its chances of undergoing plastic deformation.

Overall, the project was a success. The completion of the final design of the prototype exemplified how the basic mechanics of a split-Hopkinson pressure bar system works.

8 Acknowledgements

The senior design team 1 would like to thank all those who helped this project go from design to reality. We greatly appreciate all of their time and support because without them, this project would not have been a success. Thanks to: Dr. Hovsopian, Dr. Kosaraju, Dr. Dalban-Canassy and Dr. Shih for their guidance and support; Dr. House for sponsoring the project and helping us to better understand the principals behind it; Mr. Robert Walsh and Mr. Dustin McRae for sharing their expertise of strain gage technology and for the use of their lab at the National High Magnetic Field Laboratory; Dr. Solomon for allowing us to use the thermal fluids laboratory at the FAMU/FSU College of Engineering and Mr. Ryan Jantzen for taking time out of his busy schedule to open the doors of the thermal fluids lab so we could test our prototype using the lab's data acquisition system; Mr. Bill Starch of the Applied Superconductivity Center for machining all of our parts; Lastly, Dr. Hellstrom for giving us access to the Applied Superconductivity Center and for allowing us the use of the facility to construct our prototype.

9 Appendix

9.1.1 Detailed Budget

Detailed Budget

	Quantity	Unit Cost	Total Cost
Solenoid	1	69.94	\$69.94
T-slot Framing 1 1/2 inch (96 inch length)	2	48.15	\$96.30
Incident & Transmission Bar: 1566 Steel Bar 0.75 inch (36inch length)	2	29.42	\$58.84
T-slot Framing 1 1/2 inch (4 foot length for 6 inch braces)	1	25.15	\$25.15
Air Manifold (72 inches)	1	16.34	\$16.34
Striker Bar: 1566 Steel Bar 0.75 inch (6inch length)	2	5.17	\$10.34
Right Angle Fastener	16	4.06	\$64.96
Fasteners (Packs of 4)	16	2.71	\$43.36
Strain Gauges (Pack of 10)	3	20	\$60.00
Air Bushings 0.75 inch	4	265	\$1,060.00
Bushing Block 0.75 ID	4	135	\$540.00
0.25"x3"x72" Aluminum Sheet	1	40.35	\$40.35
0.75" Diameter x 12" Long High Tolerance Aluminum Bar	1	12.1	\$12.10
12" Aluminum U-Channel	1	14.19	\$14.19
0.75" diameter x 6" Long High Tolerance Steel Bar	1	5.26	\$5.26
Total			\$2,117.13

9.1.2 Striker Bar Velocity Calculations

The velocity of the striker bar is needed

The only requirement is that the specimen plastically deform while the incident and transmitter bars are only loaded elastically

The following equations show the process

$$\sigma_{yc} := 172 \text{MPa}$$

Yield stress of copper

$$\text{Area}_c := \pi \cdot \left(\frac{.75 \text{in}}{4} \right)^2 = 0.11 \text{in}^2$$

Area of the copper

$$F := \sigma_{yc} \cdot \text{Area}_c = 12.256 \text{kN}$$

Force Required to reach Yield

Next the mass of the steel bar is computed

$$\rho := 7.85 \frac{\text{gm}}{\text{cm}^3} = 7.85 \times 10^3 \frac{\text{kg}}{\text{m}^3}$$

Density of steel

$$v := \pi \cdot \left(\frac{0.75}{2} \right)^2 \text{in}^2 \cdot 6 \text{in} = 2.651 \text{in}^3$$

Volume of the 3/4 inch diameter, 6 inch striker bar

$$\text{mass} := v \cdot \rho = 0.341 \text{kg}$$

Mass of the striker bar

Next the amount of time the striker bar will impact the incident bar

$$c := 6100 \frac{\text{m}}{\text{s}}$$

Speed of wave propagation in steel

$$L := 6 \text{in}$$

Length of Striker bar

$$t := 2 \cdot \frac{L}{c} = 4.997 \times 10^{-5} \text{s}$$

Pressure wave propagating down the strikerbar and returning
= 2 x length/speed

$$t = 49.967 \mu\text{s}$$

Duration of impact

Finally the minimum velocity of the striker bar needed to plastically deform the specimen

$$V := \frac{F}{\text{mass}} \cdot t = 1.796 \frac{\text{m}}{\text{s}}$$

$$V = 4.017 \frac{\text{mi}}{\text{hr}}$$

Minimum velocity of striker bar needed to plastically deform the copper specimen

$$Acc := \frac{310\text{ozf}}{\text{mass}} = 252.751 \frac{\text{m}}{\text{s}^2}$$

Acceleration available from a chosen solenoid

$$L_{\text{sol}} := 1\text{in}$$

Length of piston with given force

$$D = D_0 + V_0 \cdot t + .5A_{cc} \cdot t^2$$

Generic dynamic position equation

$$\text{time}_{\text{sol}} := \left(\frac{L_{\text{sol}}}{0.5 \cdot Acc} \right)^{.5} = 0.014\text{s}$$

Derived time, from previous equation

$$V_{\text{stkr}} := Acc \cdot \text{time}_{\text{sol}} = 8.016 \frac{\text{mi}}{\text{hr}}$$

Calculated velocity from given solenoid

$$\text{Force}_{\text{striker.sol}} := \frac{V_{\text{stkr}} \cdot \text{mass}}{t} = 24.453\text{kN}$$

Maximum force transfered from solenoid

9.1.3 Comsol Analysis

ABSTRACT

It has been requested that a Kolsky bar experiment be analyzed. A Kolsky bar is a method for measuring energy absorption during plastic deformation. The physical system being built will be a shorter version of a 48 foot Kolsky bar at Eglin Air Force Base. A preliminary exercise to model and show plastic deformation and deflection due to misalignment will be accomplished. The following deliverable is this exercise. The Comsol model will use a static loading, instead of an acoustic impact load, due to the Comsol Acoustic License being unavailable to students. The static load will be the peak impact load from the experiment. The analysis shows stress in the system, beyond the yield stress of the specimen in question, thus confirming the model's accuracy. There will be an offset in the system to cause deflection, to demonstrate the need for high precision alignment

INTRODUCTION

The FAMU/FSU College of Engineering senior design group one has been tasked with upgrading a split Hopkinson bar, also known as a Kolsky bar with air bearings. This finite element analysis deliverable will model the three bars analyzed during the experiment. The Kolsky bar experiment is a method of testing energy absorbed in plastic deformation due to shock loading. The experiment is a series of four cylindrical bars all axially aligned. One bar is accelerated to a predetermined velocity; this is known as the striker bar. It then impacts the second bar. The second bar is very long and is known as the incident bar. The impact wave is then transmitted to the third bar. The third bar is the specimen being tested; it is much smaller in radius than the other three bars. Its smaller diameter multiplies the stress applied, thus plastically deforming it, before transmitting all of the energy to the fourth bar. The fourth bar is called the transmitter bar and is allowed to travel along the axis and then disburse the energy into a momentum trap. Two strain gauges are placed on the incident and transmitter bar, and data reduction methods are used to show the total energy absorbed by the specimen. The only data that is of interest is the initial impact wave. There will be modal waves, but the experiment is designed to only have the initial wave affect the plastic deformation of the specimen.

To simplify the problem only the incident bar, the specimen, the transmitter bar and the momentum trap shall be analyzed. The FAMU/FSU College of Engineering does not have an acoustics license for Comsol, and thus only a static problem can be calculated. The model will be designed around the peak load of the initial shock, and should show stresses in excess of the yield point of the copper specimen being tested. After primary analysis, a more in-depth model may be built to show effects of deflection, and maximum striker bar velocity. If an acoustics license is obtainable, the shock wave being measured with the data acquisition system can be simulated, as well as a dynamic visualization of the strain wave traveling through the entire system.

PHYSICAL SYSTEM

The relevant geometry, quantities and values of the Kolsky bar experiment are as follows:

- Diameters

- Incident Bar $D_i = 5/8 \text{ in} = 0.625 \text{ in}$
 - Transmitter Bar $D_t = 5/8 \text{ in} = 0.625 \text{ in}$
 - Specimen $D_s < 5/16 \text{ in}$
- Lengths
 - Incident Bar $L_i = 48 \text{ in}$
 - Transmitter Bar $L_t = 36 \text{ in}$
 - Specimen $L = 0.3 \text{ in}$
- Peak force from striker (Area = 1.227 in^2) = 39.566 kN
- Materials ¹
 - Incident Bar: Stainless Steel
 - $\sigma_y = 300 \text{ MPa}$
 - $c = 6100 \text{ m/s}$ (speed of sound will be relevant when studying acoustic affects)
 - Specimen: Copper
 - $\sigma_y = 70 \text{ MPa}$
 - $c = 3901 \text{ m/s}$ (speed of sound will be relevant when studying acoustic affects)
 - Transmitter Bar: Stainless Steel
 - $\sigma_y = 300 \text{ MPa}$
 - $c = 6100 \text{ m/s}$ (speed of sound will be relevant when studying acoustic affects)
- Static Loading Conditions
 - All bars in contact
 - Outside surface of momentum trap fully constrained (fixed)
 - Force applied to striker bar impact surface on incident bar
 - No roller constraints on preliminary report, to show deflection
 - Fully scaled model

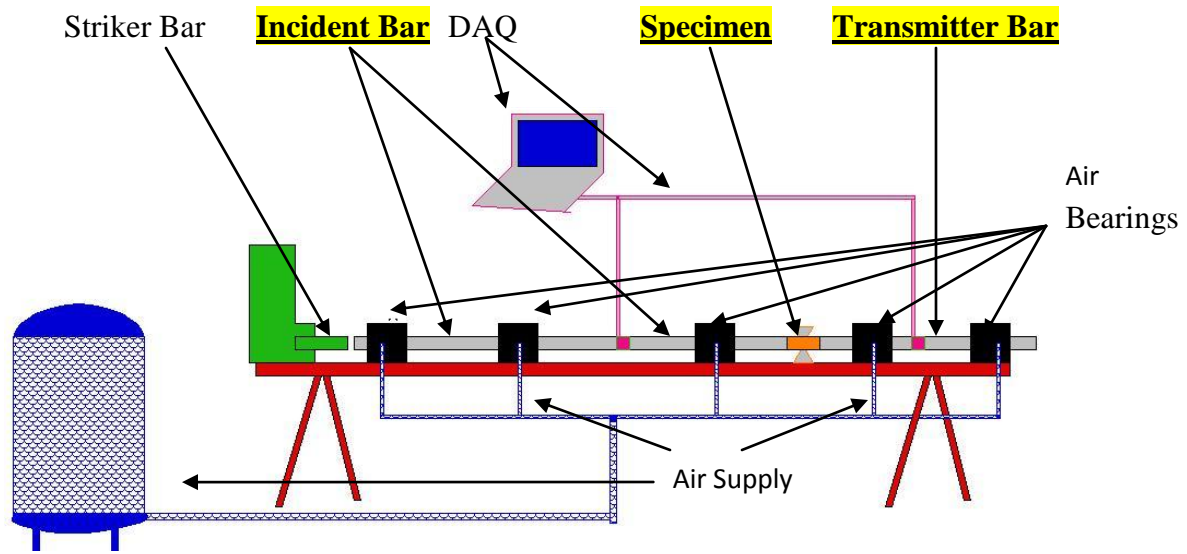


Figure 23 - Simplified graphic of Kolsky bar experiment

Please note that the pink and black sections covering the incident and transmitter bars are not discontinuities in the bar, only graphic representations of strain gauges and bearing housings respectively.

The following equation is the basic wave equation needed to develop the weak form for the system

$$\rho \cdot A \cdot \left(\frac{\partial^2 u}{\partial t^2} \right) - \frac{\partial}{\partial x} \left[\left[E \cdot A \cdot \left(\frac{d}{dt} u \right) \right] - f(x, t) \right] = 0 \quad 3$$

Where:

ρ = Density

A = Area

$\partial^2 u / \partial t^2$ = Acceleration

E = Youngs Modulus

$\partial u / \partial t$ = Velocity

f (x,t) = Square wave loading due to the striker bar

FINITE ELEMENT MODEL

The following simple finite element problem will be calculated and computed and compared to physical data:

Given:

- Kolsky bar with static loading at maximum impact load peak
- Identical geometry to physical description given previously
- Exterior boundary surface of momentum trap is fixed
- Exterior boundary surface of incident bar has applied stress of 50 MPa
- Momentum trap is shaped to create displacement due to applied stress
- Materials chosen are Comsol's built in Steel AISI 4340 and Copper
- Assumed that static loading at peak impact load will give similar results to actual shock wave loading

RESULTS

The following figures show the to-scale model of the system.



Figure 24 - Fully scaled Comsol image of Kolsky bar before loading

Please note the relative size of the sample, to the length of the incident and transmission bar, as well as the offset of the momentum trap.

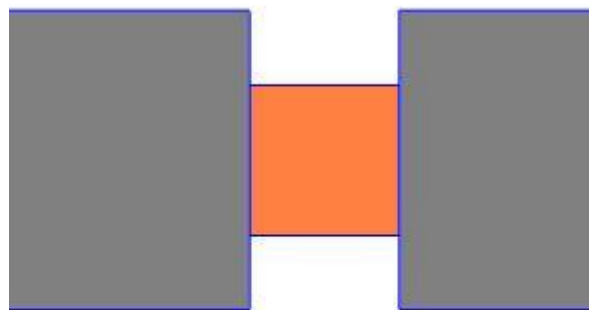


Figure 25 - Detail of sample and interface with incident and transmitter bars.

Color difference denotes material difference. Gray color is for stainless steel, while orange represents copper. Please note the reduction in diameter for the purpose of multiplying stress in the copper.



Figure 26 - Detail of momentum trap. Please note the offset of the momentum trap.

The simulation was then run and the static results are very well matched to the given data. The stress shown in figure 5 gives a maximum stress in the copper of greater than 100 MPa. The given yield stress of copper is around 70 MPa. Thus the copper will have plastically deformed. The maximum stress in the steel is around 70 MPa, which is less than half of the yield strength of steel at 300 MPa, which prevents fatigue failure, allowing the system to be used indefinitely ².

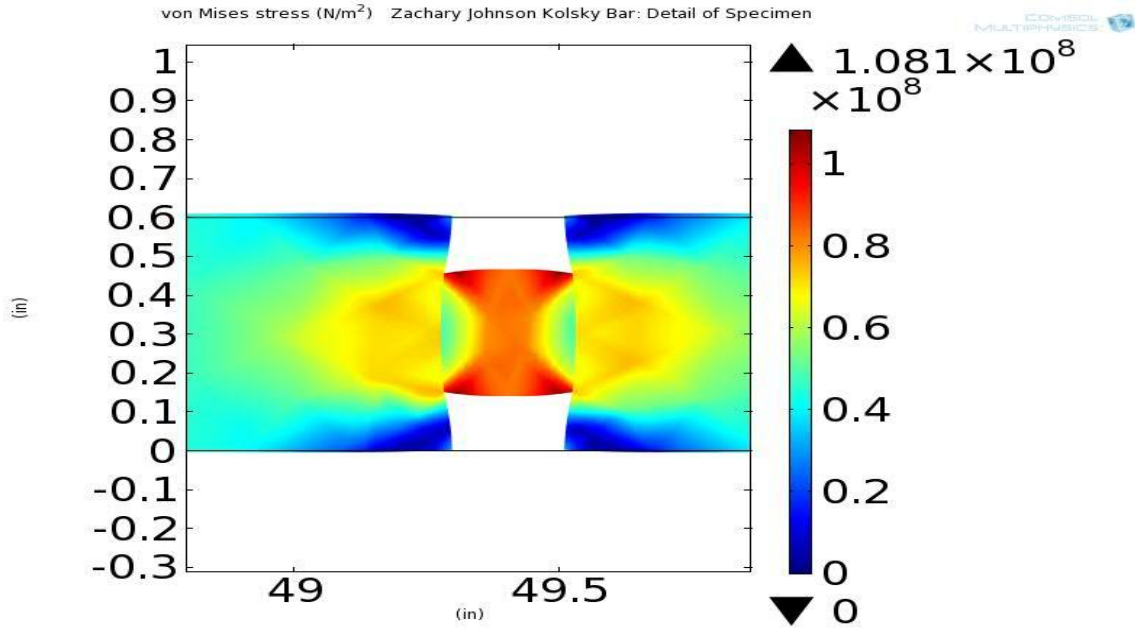


Figure 27 - Stress in the incident bar, specimen and transmitted bar with static loading

The contour line graph shown in figure 6 shows how the maximum strain develops. Deformation occurs most abruptly at the boundaries with the larger diameter steel bars, which again conforms to the actual experiments.

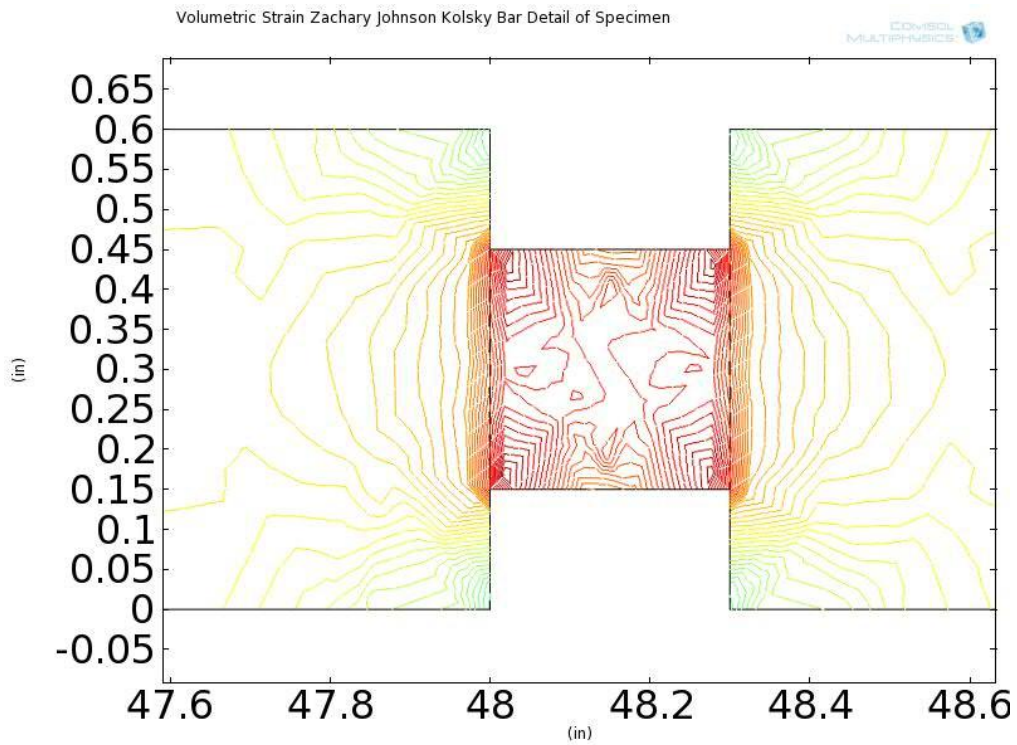


Figure 28 - Strain in the incident bar, specimen and transmitted bar

The image in figure 7 is the deflection in the incident bar caused by the uneven stress and strain in the offset momentum trap shown in figure 8. This deflection shows the need for very high precision alignment, which is a design request for the senior design project.

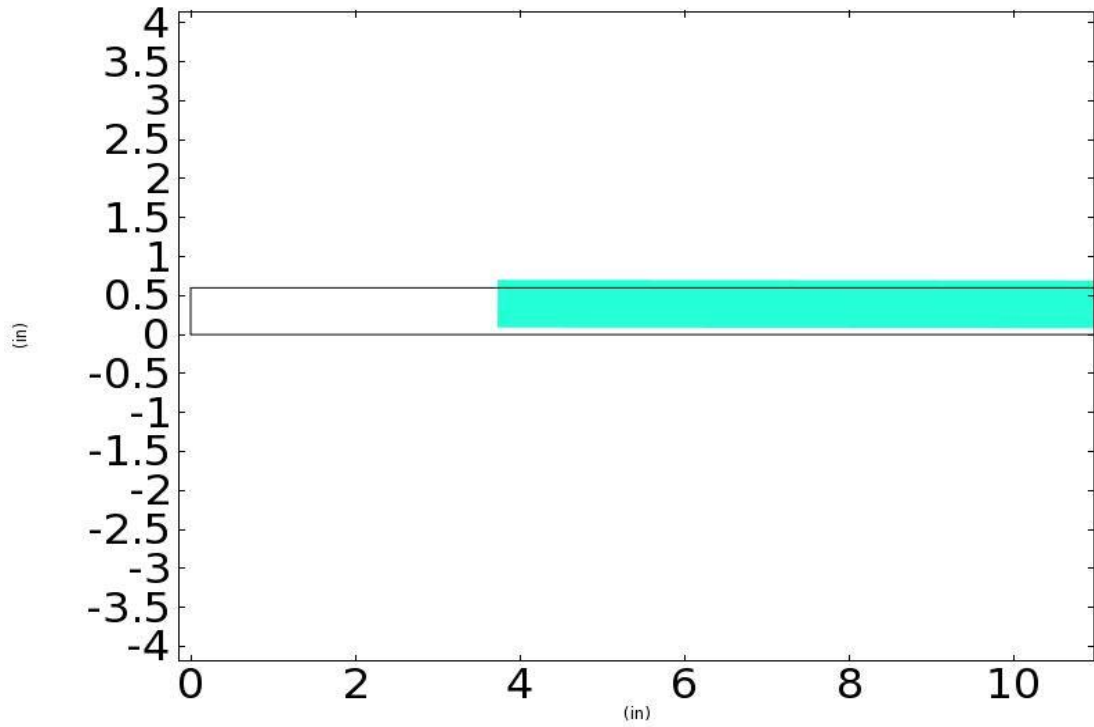


Figure 29 - Deflection in the incident bar

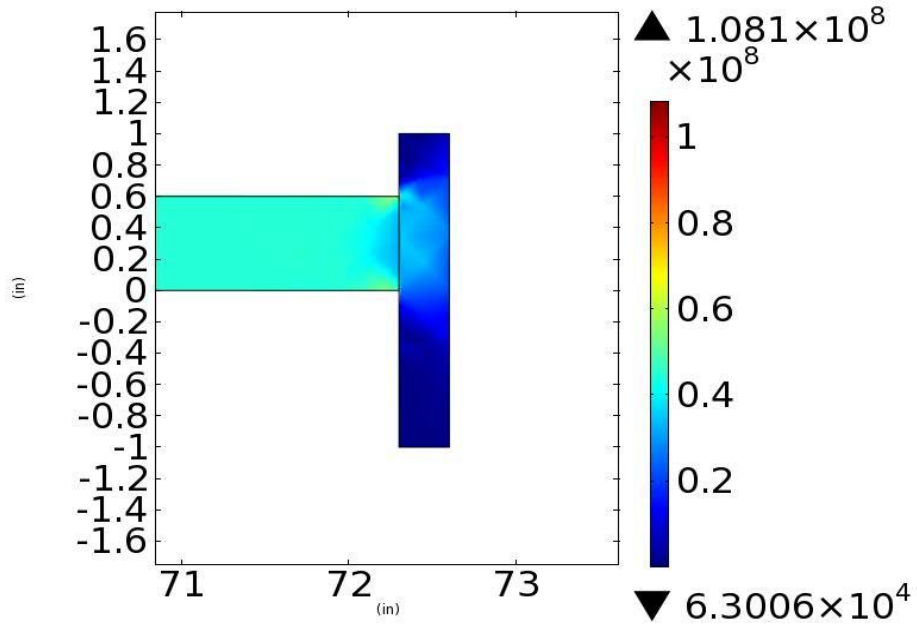


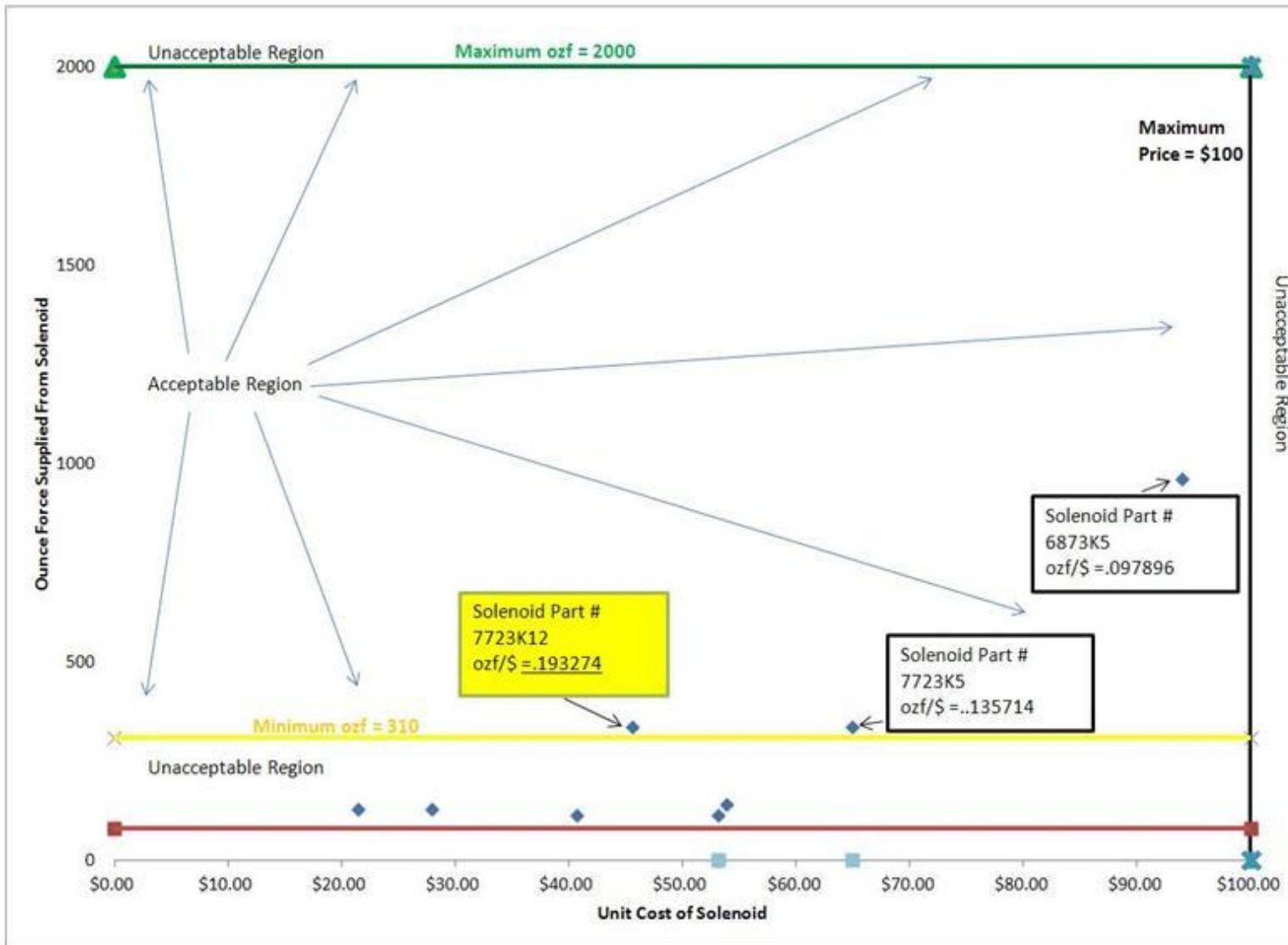
Figure 30 - Stress developed in the momentum trap

DISCUSSION

The results given in this deliverable are very much as expected. The copper specimen has been loaded past the point of yield, which gives the desired plastic deformation. The deflection has been shown which gives graphical representation of the need for high precision alignment, as requested.

However, improvement can be made. Strain gauges are to be placed on the physical system, and could be modeled by having a time dependent force applied to the Comsol system. If an acoustics license is acquired, then the wave analysis, energy absorption, strain rate, and other properties could be analyzed.

9.1.4 Solenoid Optimization



9.1.5 Mathematics and Analysis Methods

For the design of any engineered metallic item in which the behavior of the material under static or dynamic loading is significant, a statistically relevant reproducible trend. To begin, the force applied has to be standardized through a force/material density. Assuming the force is only in one direction, the stress through a unit of area is given as:

$$\sigma = F/A$$

where σ = stress

F = force

A = instantaneous area

In cases of loading where the change in the length of the material under loading is needed the change in length is given as a percentage of the initial length as:

$$\varepsilon = (L_i - L_o) / L_o$$

where ε = strain

L_i = instantaneous length

L_o = initial length

The SHPB experiment loads three piece of metal in two different ways. The incident and transmitter bar are loaded elastically. See the SHPB section for more detail. That is the loading occurs and the material stretches or compresses and then after the loading ceases, the material returns to its original length, with no permanent crystal deformation, or “slip” along the microscopic planes of atoms. The point at which the material begins to permanently deform is called the yield point. Inside of the elastic region of deformation the relationship between stress and strain is linear. The ratio of this relationship is specific to each material. This ratio is called the Young’s Modulus E given as:

$$\sigma = E * \varepsilon$$

This elastic behavior is necessary for the SHPB experiment to be quantified. The measurement taken from each of the elastically loaded bars is the strain ε . The strain is measured by a strain gauge. A strain gauge uses the physical changes caused by strain to be measured as a change in resistivity in a resistor set. The strain gauge has a ratio of the

change in resistance divided by the strain passing through the material being tested. This ratio is called the gauge factor and is given as:

$$GF = [(R_i - R_g) / R_g] / \epsilon$$

Where GF = gauge factor

R_i = instantaneous resistance

R_g = initial resistance

ϵ = strain

So therefore if the desired strain at a given time is desired, one can rearrange the equation to be:

$$\epsilon = [(R_i - R_g) / R_g] / GF$$

Where GF = gauge factor

R_i = instantaneous resistance

R_g = initial resistance

ϵ = strain

This allows the strain to be the output of the given input of R_i from the resistor set.

The resistor set is based on a Wheatstone circuit. This circuit allows for precise measurements of the resistance inside of the stress gauge resistor. The Wheatstone circuit contains four resistors, three of which have resistances of known value, and one is the stress gauge resistor. The relationship between them is as follows

$$R_g = (R_2 / R_1) * R_3$$

Where R_g = stress gauge resistance

R_1 , R_2 and R_3 are known resistances.

The voltage difference between the two interior junctions is the measured output.

The governing equation is given as follows:

$$V_g = [(R_g / \{ R_3 + R_g \}) - (R_2 / \{ R_1 - R_2 \})] * V_a$$

Where V_g = measured voltage

R_g = stress gauge resistance

R_1 , R_2 and R_3 = known Resistances

V_a = applied voltage

This instantaneous strain is recorded with respect to time. This measurement is taken in two places: The incident bar and the Transmitter bar. The gauges give three strain wave measurements: 1) an Incident wave through the incident bar ϵ_I 2) A reflected wave through the incident bar ϵ_R and 3) An incident wave through the transmitter bar ϵ_T . Given that the initial length of the specimen and the speed of sound through the specimen material are known, then both the average engineering strain rate as well as the total strain can be calculated using the following equations:

$$d\epsilon_{avg} / dt = (C_b / L_s) * (\epsilon_I - \epsilon_R - \epsilon_T)$$

where $d\epsilon_{avg} / dt$ = average engineering strain rate

L_s = initial length of the specimen.

$$\epsilon_s = (C_b / L_s) * \int_0^t [(\epsilon_I - \epsilon_R - \epsilon_T) * dt]$$

where ϵ_s = strain in the specimen

As discussed before the strain must have a corresponding stress to allow for computation of the Young's Modulus. The stress at the connection between the incident bar and the specimen is given as a ratio of the area of the two bars (as energy is conserved, the force that is transmitted through the large area of the incident bar must be transmitted into the small area of the specimen) the Young's modulus of the Incident bar and the Incident and Reflected waves as:

$$\sigma_1 = (A_B / A_s) * E_B * (\epsilon_I + \epsilon_R)$$

The stress at the connection between the specimen and the transmitter bar is similar to before, but only the transmitted wave is taken into account as:

$$\sigma_2 = (A_B / A_s) * E_T$$

From this the average stress can be taken:

$$\sigma_{avg} = 0.5 * (\sigma_1 + \sigma_2)$$

The elastic strain energy in the incident bar due to the incident wave is given as :

$$E_I = 0.5 * A_B * C_B * E_B * T * \epsilon_I^2$$

Where E_I = strain energy due to the incident wave

A_B = cross sectional area of the bar

C_b = Speed of sound in the bar

T = amount of time the square loading wave was applied through the gauge.

The elastic strain energy is the same for the reflection and transmitted wave:

$$E_I = 0.5 * A_B * C_B * E_B * T * \epsilon_R^2$$

$$E_I = 0.5 * A_B * C_B * E_B * T * \epsilon_T^2$$

The strain energy used in the deformation of the specimen is given as

$$\delta S_E = E_I - E_R - E_T$$

The Kinetic energy is the energy of motion. The kinetic energy being transmitted by the waves are given as:

$$K_I = 0.5 * \rho_B * A_B * C_B^3 * T * \epsilon_I^2$$

$$K_R = 0.5 * \rho_B * A_B * C_B^3 * T * \epsilon_R^2$$

$$K_T = 0.5 * \rho_B * A_B * C_B^3 * T * \epsilon_T^2$$

The strain energy used in the deformation of the specimen is given as:

$$\delta K_E = E_I - E_R - E_T$$

The total deformation energy in the specimen is given as:

$$E_s = 2 * \delta K_E = 2 * \delta S_E$$

STRAIN GAUGES

The strain gauges used in the SHPB experiment are electrical resistance gauges. They use the physical distortion in the width of the electrical conductors. The thinner the conductor becomes the more resistance it creates. The thicker the conductor becomes, the less resistance it creates. The placement of the strain gauge is such that as the material being tested is put into tension, the lengths of the gauge are being stretched and as such the resistance increases. If the material is put into compression, then the lengths of the gauge are being shortened and as such the resistance decreases.

The strain gauge has a ratio of the change in resistance divided by the strain passing through the material being tested. This ratio is called the gauge factor and is given as:

$$GF = [(R_i - R_g) / R_g] / \epsilon$$

Where GF = gauge factor

R_i = instantaneous resistance

R_g = initial resistance

ϵ = strain

So therefore if the desired strain at a given time is desired, one can rearrange the equation to be:

$$\epsilon = [(R_i - R_g) / R_g] / GF$$

Where GF = gauge factor

R_i = instantaneous resistance

R_g = initial resistance

ϵ = strain

This allows the strain to be the output of the given input of R_i from the resistor set.

The resistor set is based on a Wheatstone circuit. This circuit allows for precise measurements of the resistance inside of the stress gauge resistor. The Wheatstone circuit contains four resistors, three of which have resistances of known value, and one is the stress gauge resistor. The relationship between them is as follows

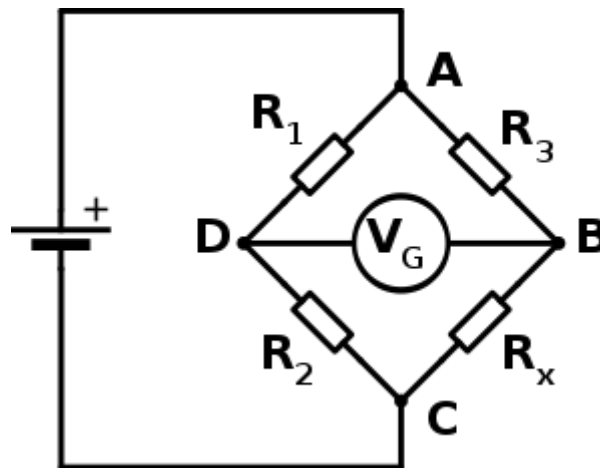


Figure 31 - Wheatstone bridge

$$R_x = (R_2 / R_1) * R_3$$

Where R_x = stress gauge resistance

R_1 , R_2 and R_3 are known resistances.

The voltage difference between the two interior junctions is the measured output. The governing equation is given as follows:

$$V_g = \left[\left(\frac{R_g}{R_3 + R_x} \right) - \left(\frac{R_2}{R_1 - R_2} \right) \right] * V_a$$

Where V_g = measured voltage,

R_x = stress gauge resistance

R_1 , R_2 and R_3 = known resistances

V_a = applied voltage

Air Bushings

Although the name of this project implies the use of air bearings, what were actually used in the final design were air bushings. An example of an air bearing is the surface of a air hockey table which allows for reduced friction while still permitting 3 degrees of freedom (2 linear and 1 rotational) to an object passing over its surface while and air bushing restricts a rod's movement to linear motion along and rotational motion about the rod's lengthwise axis.

There were a number of types of air bushings to choose from so the type most suitable to this project was needed to be determined. The main distinction between types of air bushings is the method by which compressed air is supplied to the 'contact' surface between the bushing and rod. The most basic method is the placement of one or more small outlets in the contact surface. This method can be modified to include shallow channels in the contact surface which guide the compressed air away from the outlets in order to achieve a more uniform pressure distribution. The method which provides the most even pressure distribution involve the use of an air-permeable material, such as porous carbon, to distribute the compressed air along the entirety of the contact surface.

Air Supply

Given that air bushings are used in this project, the method by which those bushings are to be supplied with compressed air must also be addressed. The main air supply for the system was chosen to be a tank of pressurized Argon which is non-reactive and has been filtered to beyond 99% pure. New Way Air Bearings, the type chosen for

use in this project, produces an air bushing for 0.75 inch diameter rods which requires a flow rate of 7.0 to 9.60 Standard Cubic Feet per Hour (SCFH) and utilizes a porous contact surface.

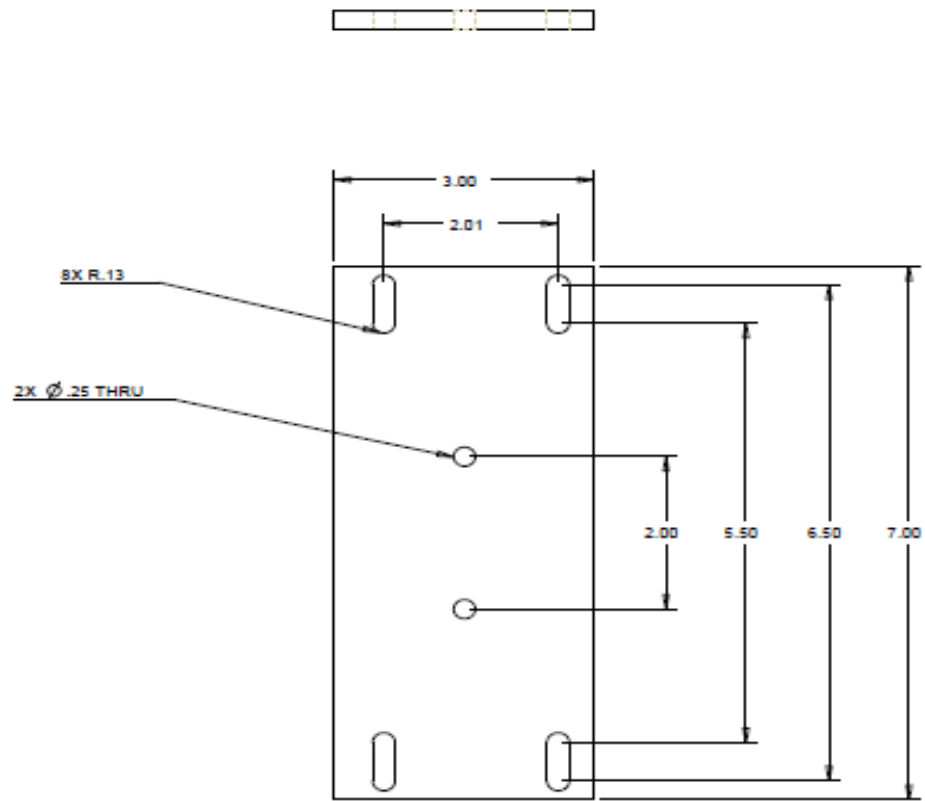
Strain Gauges

Strain gauges are devices used to measure the amount of deformation in object when a force has been applied to it. The values measured for strain are usually less than 0.005 and are displayed in units of micro-strain. Strain can be measured for tensile or compressive loads. The strain which will be measured during the course of this project's experimentation is due to compressive loading. A strain gauge works by converting mechanical movement into an electrical signal through a change in capacitance, inductance, or resistance. In this experiment the strain gauge will respond to the change in resistance.

10 Engineering Drawings

See the following pages.

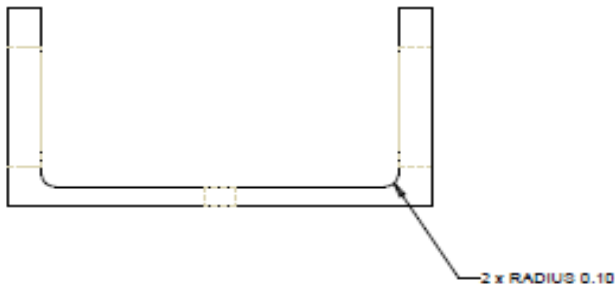
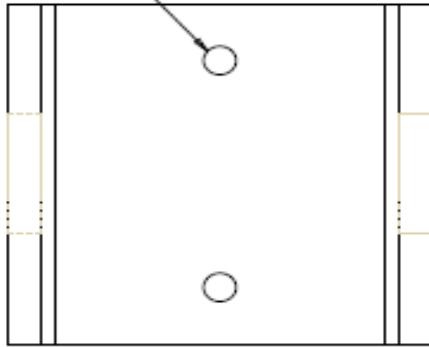
NOTE: NEED TWO OF THIS PART



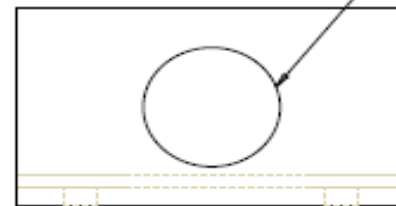
FAMU/FSU COLLEGE OF ENGINEERING
SENIOR DESIGN GROUP 1
FEBRUARY 23, 2012
STRIKER BAR BASEPLATE

ALL DIMENSIONS ARE IN INCHES

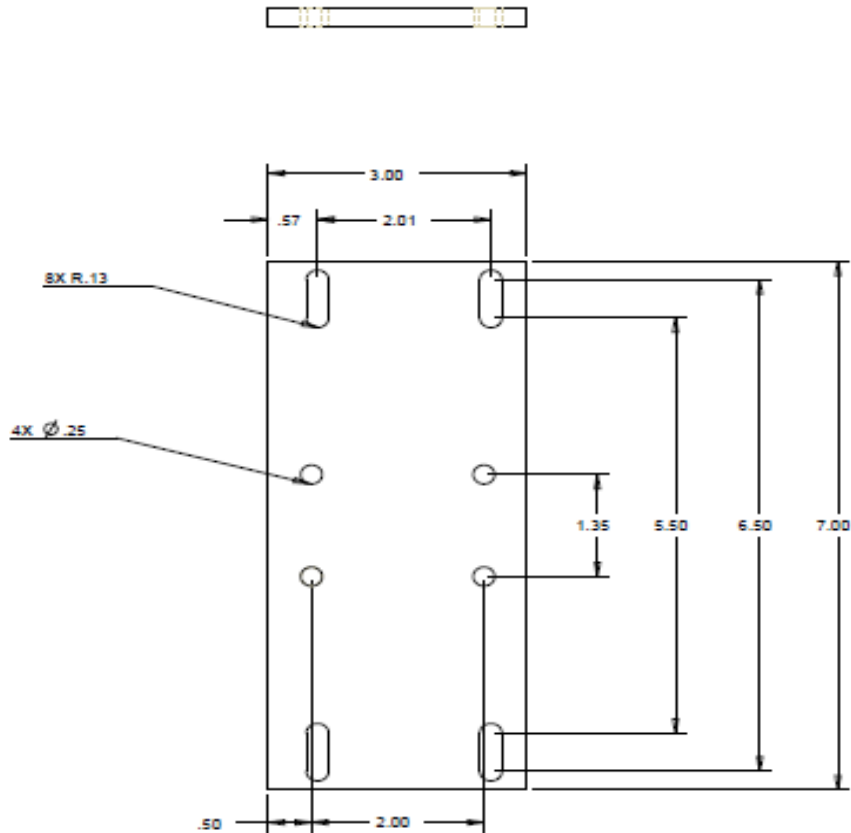
2 HOLES DIAMETER 0.25 THRU



2 HOLES DIAMETER 1.05 THRU

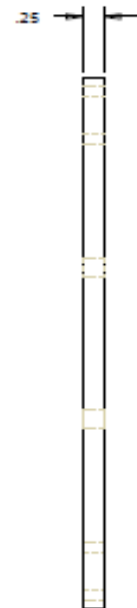
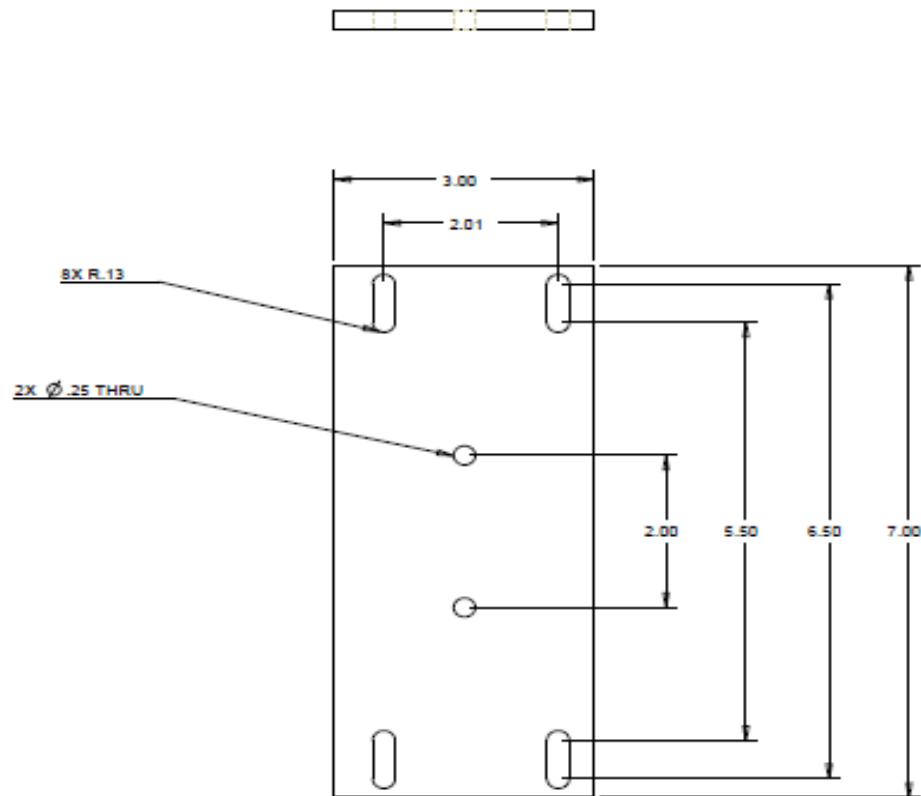


FAMU-FSU COLLEGE OF ENGINEERING
SENIOR DESIGN GROUP 1
2/23/2012
U CHANNEL STRIKER



FAMU/FSU COLLEGE OF ENGINEERING
 SENIOR DESIGN GROUP 1
 FEBRUARY 23, 2012
 SOLENOID BASEPLATE

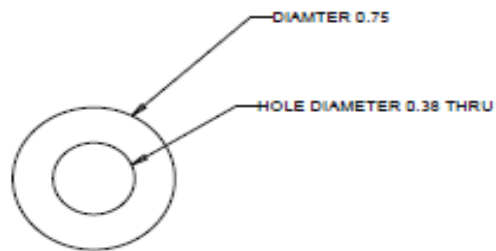
NOTE: NEED TWO OF THIS PART



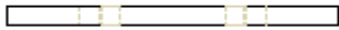
FAMU/FSU COLLEGE OF ENGINEERING
SENIOR DESIGN GROUP 1
FEBRUARY 23, 2012
STRIKER BAR BASEPLATE



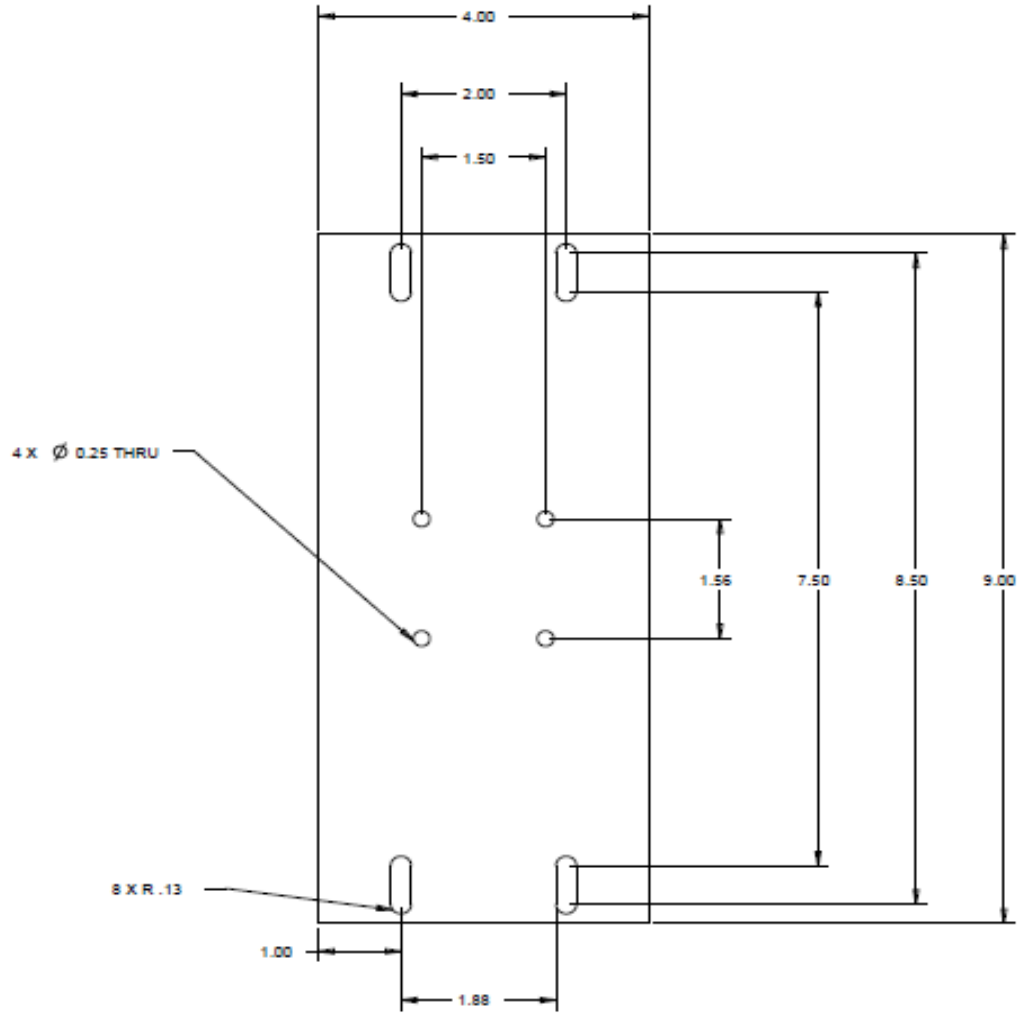
ALL DIMENSION ARE IN INCHES



FAMU-FSU COLLEGE OF ENGINEERING
SENOIR DESIGN GROUP 1
2/23/2012
LASER HOLDER

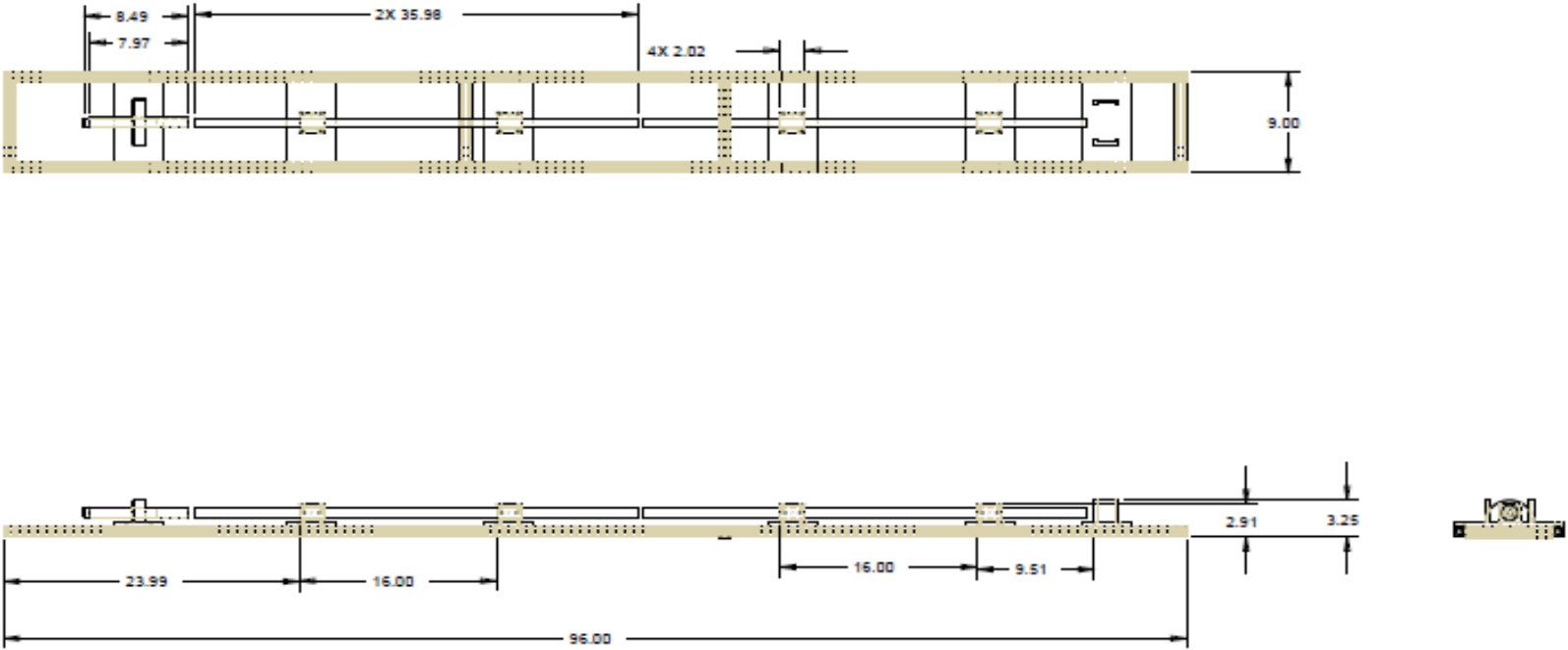


ALL DIMENSIONS ARE IN INCHES



FAMU-FSU COLLEGE OF ENGINEERING
SENIOR DESIGN GROUP 1
APRIL 5, 2012
BUSHING BLOCK PLATE

ALL DIMENSIONS ARE IN INCHES



FAMU-FSU COLLEGE OF ENGINEERING
SENIOR DESIGN GROUP 1
APRIL 5, 2011
SHPB ASSEMBLY

11 References

- NewWayAirBearings. "Porous Media Technology." *New Way Air Bearings*. Web. 09 Oct. 2011. <<http://www.newwayairbearings.com/Porous-Media-Technology>>.
- New Way Air Bearings, Inc. *Porous Media Air Bearing Solutions*. Aston: New Way Air Bearings, 2010. *New Way Air Bearings*. 2010. Web. 9 Oct. 2011. <http://www.newwayairbearings.com/adx/asp/adxGetMedia.aspx?DocID=19,16,12,3,1,Documents&MediaID=5010&Filename=new_way_line_brochure_air_bushings_combined_nwab-10-m-037-v05-2010-05-17-2500_page.pdf>.
- "SCFM versus ACFM and ICFM." *Engineering ToolBox*. Web. 09 Oct. 2011. <http://www.engineeringtoolbox.com/scfm-acfm-icfm-d_1012.html>.
- "Care and Air." *New Way Air Bearings*. Web. 09 Oct. 2011. <<http://www.newwayairbearings.com/Care-And-Air>>.
- Omega Engineering Inc. (n.d.). Practical Strain Gauge Measurements.
- Omega Engineering. "The Strain Gauge". *Omega Engineering*. 09 Oct. 2011. <<http://www.omega.com/literature/transactions/volume3/strain.html>>
- "Strain Gauge." Wikipedia, the Free Encyclopedia. Web. 26 Oct. 2011. <http://en.wikipedia.org/wiki/Strain_gauge>.
- Chen, Weinong W., and Bo Song. Split Hopkinson (Kolsky) Bar: Design, Testing and Applications. New York: Springer Verlag, 2010. Print.
- "Electrical Strain Gauges." This Is Bits.me.berkeley.edu. Web. 26 Oct. 2011. <http://bits.me.berkeley.edu/beam/sg_2a.html>.

- "Capacitance Measurement Systems: Non-contact Measurement Sensors, Solutions and Systems –
- MTI Instruments." Non-contact Measurement Sensors, Solutions and Systems, Laser, Fiber Optic & Capacitance Sensors - MTI Instruments. Web. 26 Oct. 2011. <<http://www.mtiinstruments.com/products/capacitancemeasurement.aspx>>.
- "Micron Instruments - Bar Gage." Micron Instruments - Corporate Home Page. Web. 26 Oct. 2011. <<http://www.microninstruments.com/store/bargage.aspx>>.
- Green, Thomas M. "MatLab Intro. Thomas M. Green." Web. 26 Oct. 2011. <<http://www.contracosta.edu/legacycontent/math/Lmatlab.htm>>.
- "NI LabVIEW - Improving the Productivity of Engineers and Scientists." National Instruments: Test, Measurement, and Embedded Systems. Web. 26 Oct. 2011. <<http://www.ni.com/labview/>>.
- "Air Bushings." New Way Air Bearings. 21 October 2011. <http://www.newwayairbearings.com/Default.aspx?DN=e05778a6-99a1-402c-9073-c9c95e516d41>.
- "Mounting Components." New Way Air Bearings. 21 October 2011. <<http://www.newwayairbearings.com/Mounting-Components/>>
- "Metals" Online Metals. 22 October 2011. <<http://www.onlinemetals.com/>>
- McMaster-Carr. McMaster-Carr. Web. 26 Oct. 2011. <<http://www.mcmaster.com/>>.
- Faztek. Faztek, LLC. Web. 26 Oct. 2011. <<http://faztek.rtrk.com/?scid=1322663>>.

- "ThinkGeek :: Blue Violet Laser Pointer." ThinkGeek :: Stuff for Smart Masses. Web. 26 Oct. 2011. <<http://www.thinkgeek.com/gadgets/lights/b847/>>.
- NorthernTool. "Klein Tools Rare Earth Magnet Torpedo Level —9in., Model# 931-9RE | Torpedo Levels |
- Northern Tool Equipment." Portable Generators, Pressure Washers, Power Tools, Welders | Northern Tool Equipment. Web. 26 Oct. 2011. <http://www.northerntool.com/shop/tools/product_200357997_200357997>.
- "Red Laser Pointer Torch Key Chain Fantastic as a Star-pointer - Easily Visible at Night Time." Laptop Battery Online, Battery Charger And Electronic Accessories Factory. Web. 26 Oct. 2011. <<http://www.my-batteries.net/laserpointer/red-laser-pointer-with-key-chain.htm>>.
- "Light Gas Gun." Wikipedia, the Free Encyclopedia. Web. 27 Oct. 2011. <http://en.wikipedia.org/wiki/Light_gas_gun>.
- Toolbox, Engineering. Speed of Sound in Some Common Solids. *www.EngineeringToolBox.com*. [Online] [Cited: 11 3, 2011.] <https://pod51010.outlook.com/owa/?rru=home>.
- Norton, Robert L. *Design of Machinery*. New York, Ny : McGraw-Hill, 2003.
- Reddy, J.N. *An Introduction to the Finite Element Method*. New York, NY : McGraw-Hill, 1984.

12 Biographies

Team Leader - Donald Hayes II:

Donald Hayes II was born and raised in the beautiful town of Eustis, Florida, and is a graduating senior in Mechanical Engineering at Florida A&M University. It is his dream to pursue a job in the aerospace industry after graduation as well as obtain a Master's degree. His experience includes a summer internship with The Boeing Company, in Cape Canaveral Florida. In his spare time, he enjoys playing basketball and golf.

Team Secretary – Joseph Chason:

Joseph Chason is currently a senior in Mechanical Engineering at Florida State University from Perry, Florida. After graduating this spring, he plans to continue his education at FSU and pursue a Master's in Mechanical Engineering through the BS-MS program. While he has been at FSU, he has had two internships, one with Buckeye Technologies Inc. and one with Eglin Air Force Base. During his leisure time away from school, he enjoys reading, playing his violin and mandolins, and spending time with his friends and family. When an opportunity arises, he also enjoys kayaking, fishing, hunting, paintball, camping and horseback riding.

Team Secretary – Zachary Johnson:

Zack Johnson is currently a senior in Mechanical Engineering at FSU. He received a B.S. Degree in Business Management from Chipola College in 2010. He is currently doing additional research at the Applied Superconductivity Center here at FSU as well as working full time as a butcher in his home town. He plans on beginning graduate school for Materials Science starting in the fall of 2012. Aside from school and work, he is very passionate about playing guitar and reading.

Team Liaison – Sarah Napier:

Sarah Napier is a senior FSU student in Mechanical Engineering at the FAMU/FSU College of Engineering. While obtaining her Bachelors of Science degree, she also work as a research assistant at the National High Magnetic Field Laboratory in the Magnet Science and

Technology department with some of the finest engineers and scientists around. At the magnet lab, she creates 2D and 3D CAD drawings and models of various magnet components as well as performing stress analysis calculations for support stands. After graduation in the spring, she plans to enter the work force as a mechanical engineer and eventually go back to school to obtain a Master's in Business Administration. Outside of school and work, she is a competitive horseback rider in the sport of dressage. She also raises, trains and shows Miniature Horses and Shetland Ponies with her parents in Jacksonville, Florida.